ARTICLE

Magnetic anisotropies and slow magnetic relaxation of three tetrahedral tetrakis(pseudohalido)-cobalt(II) complexes

Received 00th January 20 xx, Accepted 00th January 20 xx

DOI: 10.1039/x0xx00000x

Shu-Yang Chen,^a Wei Lv,^a Hui-Hui Cui,^a Lei Chen,^b Yi-Quan Zhang,^{c*} Xue-Tai Chen,^{a*} Zhenxing Wang,^{d*}, Zhong-Wen Ouyang,^d Hong Yan^{a*} and Zi-Ling Xue^e

Three mononuclear tetrakis(pseudohalido)-cobalt(II) complexes $(Ph_4P)_2[Co(N_3)_4] \cdot 0.5H_2O$ (1) and $(Ph_4P)_2[Co(E)_4]$ (E = NCO⁻, 2; NCS⁻, 3) were synthesized and structurally characterized. Each compound contains a distorted tetrahedral Co²⁺ ion coordinated by four pseudohalide ligands. Their magnetic properties have been studied by direct-current magnetic measurements and high-frequency and -field EPR spectroscopy (HFEPR), suggesting the easy-axis magnetic anisotropy for 1 and 2, but easy-plane anisotropy for 3. The analyses of HFEPR data yielded *D* values of -5.23 and +3.63 cm⁻¹ for 2 and 3, respectively. The absence of the EPR signal in 1 is consistent with the negative sign and large value of zero-field splitting (ZFS) parameter *D* in 1. The nature of magnetic anisotropies of 1-3 have also confirmed by the ab-initio calculations. The calculated *D* values are well consistent with those determined by magnetometry and HFEPR studies. Alternating-current (ac) magnetic susceptibilities reveal the slow magnetic relaxation under an applied magnetic field and thus 1-3 are field-induced single-ion magnets (SIMs).

Introduction

Single-molecule magnets (SMMs), which display slow magnetic relaxation, have been intensively studied in the last three decades because of their potential applications in quantum computation, high density information storage and molecular spintronics. The initial research effects have been focused on SMMs based on polynuclear metal complexes since the discovery of the first SMM Mn₁₂-acetate. The subsequent studies prove difficult to simultaneously enhance magnetic anisotropy and enlarge spin number for these polynuclear complexes, which are responsible for the SMM properties. Recent studies have turned to the SMMs containing a single paramagnetic ion, which are referred to as single-ion magnets (SIMs). Compared to the extensively studied lanthanide ion SIMs, d-ion SIMs exhibit the lower energy barrier for spin reversal due to their weak magnetic

anisotropies. However a *d*-ion SIM provides a better model to fine-tune magnetic anisotropy through adjusting the nature of donor atoms, coordination number and geometry. To date, various transition metal complexes containing 3*d* ions⁵⁻¹⁵ have displayed slow magnetic relaxation, among which Co(II)-based SIMs is the largest family with various coordination configurations and coordination numbers from two to eight.⁵⁻¹⁵

Four-coordinate tetrahedral Co(II)-based SIMs are particularly attractive. 8-11 The tetrahedral geometry splits the *d* orbitals of the Co(II) ion to produce a small energy gap between the ground and excited states, facilitating the spin-orbit coupling and thus promoting magnetic anisotropy. 8-11 The four-coordinate Co(II)-SIMs usually contain a mixed donor set from N, P, As, O, S, Se or halides. A smaller number of homoleptic SIMs containing a CoX4 core (X = O, S, Se, Te, 9 N, 10 Cl¹¹) with same four ligands, which are summarized in Table S1 (ESI†), have been reported. Since mixed ligands in a complex could induce additional anisotropy arising from the difference between the ligands and the chelating effect, homoleptic four-coordinate Co(II) complexes could be better models to study the magneto-structural correlations.

The nature of donor atoms has been shown to tune magnetic anisotropy. In this regard, several studies have been performed on the effect of the donor atoms of the congeners on the magnetic anisotropy. $^{8c\text{-}8g,9b}$ Specifically, the effect of pseudo-halide ligands on magnetic properties of Co(II) complexes have been investigated. 8f,16 Switlicka *et al.* found easy-axis anisotropy for [Co(bmin)₂(L)₂] (bmin = 1-benzyl-2-methylimidazole,, L = NCS⁻) and easy-plane anisotropy for the analogues with L = NCO⁻, N₃⁻ in these three field-induced SIMs using the magnetometry and theoretical calculations. 8f Krzystek

Electronic Supplementary Information (ESI) available: XRD patterns, calculation results and magnetic data. See DOI: 10.1039/x0xx00000x

^{a.} State Key Laboratory of Coordination Chemistry, School of Chemistry and Chemical Engineering, Nanjing University, Nanjing 210023, China. E-mail: xtchen@nju.edu.cn; hyan1965@nju.edu.cn

b. School of Environmental and Chemical Engineering, Jiangsu University of Science and Technology, Zhenjiang 212003, China.

c- Address here. Jiangsu Key Laboratory for NSLSCS, School of Physical Science and Technology, Nanjing Normal University, Nanjing 210023, China. Email: zhanqviquan@ninu.edu.cn

d-Wuhan National High Magnetic Field Center & School of Physics, Huazhong University of Science and Technology, Wuhan 430074, China. Email: zxwana@hust.edu.cn

e. Department of Chemistry, University of Tennessee, Knoxville, Tennessee 37996, USA.

et al. have revealed the sensitivity of the ZFS parameter D values in the series of complexes TpR,R'CoL (TpR,R'- = hydrotris(3-R,5-R'-pyrazol-1-yl)borate anion, L= NCS-, NCO-, N₃-) by HFEPR. ¹⁶

Magnetic properties of tetrakis(pseudohalido)-cobalt(II) complexes have attracted considerable interest. 10e-10h Recently Gao et al. reported slow magnetic relaxation in two Co(II)-SIMs containing the $[Co(NCS)_4]^{2\text{-}}$ anion, $\,[K(C_{12}H_{24}O_6)]_2\,[Co(NCS)_4]\,$ and [Ba(C₁₂H₂₄O₆)·3H₂O][Co(NCS)₄], which exhibit weak easy plane anisotropies with D values of +2.57 and +5.56 cm⁻¹ determined by HFEPR. 10e Later, magnetic anisotropies and magnetic relaxation were revealed for complexes with the same magnetic anions but square-planar [Ni(Me₆trans[14]dieneN₄)]²⁺ cations^{10f} and a spin-crossover Co(II) cation [Co(Brphterpy)₂]²⁺, whose D values were estimated to be positive. ^{10g} Similarly, the analogous anion [Co(NCO)4]2- containing a spin-crossover cation [Co(tppz)₂]²⁺ exhibits a weak easy-plane anisotropy with a D value of +4.3 cm⁻¹ and is a field-induced SIM. ^{10h} However, the analogous [Co(NCS)₄]²⁻ anion with the same [Co(tppz)₂]²⁺ cation is not a field-induced SIM. 10h These reported examples of complexes with the [Co(NCS)₄]²⁻ and [Co(NCO)₄]²⁻ anions are summarized in Table S2 (ESI). Except the ZFS parameters of the first two complexes $[K(C_{12}H_{24}O_6)]_2[Co(NCS)_4]$ [Ba(C₁₂H₂₄O₆)·3H₂O][Co(NCS)₄] determined by HFEPR spectra, the other complexes were only estimated by the fitting of magnetic data. It is noted that that the D and E values varies with the associated cations.

It is known that the counter-ion has an effect on magnetic property especially the SMM property of SIMs. Besides, the azido ligand is also an important pseudohalide. 12b However, the magnetic property of the tetrakis(azido)-Co(II) anion has been not studied yet. We have prepared and characterized three four-coordinate Co(II) complexes with the same cation Ph₄P⁺, (Ph₄P)₂[Co(N₃)₄]·0.5H₂O (1) and (Ph₄P)₂[Co(E)₄] (E = NCO⁻, 2; NCS⁻, 3). They have similar tetrahedral geometries with isostructural CoN₄ core with the nitrogen atoms from the pseudohalide ligands. Detailed direct-current (dc) magnetic measurements and HFEPR spectra have been used to study their magnetic anisotropies. The ac magnetic susceptibility studies show that 1-3 are field-induced single-ion magnets. The results are reported herein.

Experimental Section

General information

All starting reagents were used as received from commercial sources without further purification. The infrared spectra were measured in the range of 400-4000 cm⁻¹ on a Tensor 27 FT-IR spectrometer using KBr pellets. Elemental analyses (C, H, and N) were performed on an Elementar Vario ELIII elemental analyzer. The powder XRD patterns were recorded on a Bruker D8 Advance X-ray powder diffractometer at a voltage of 40 kV and a current of 40 mA in the 2θ range of 5-50° at room temperature (Figs. S1-S3, ESI). High-frequency and -field EPR (HF-EPR) experiments were performed using a spectrometer constructed at the National High Magnetic Field Laboratory, USA. 17

Caution! Azide salts of metal complexes are potentially explosive and should be handled in small quantities with care.

Synthesis of [Ph4P]2[CoCl4]. This compound was synthesized according to the published procedure. ¹⁸ A solution of Ph4PCl (0.75 g, 2.0 mmol) in ethanol (3 mL) was added under stirring to a solution of CoCl2·6H2O (0.24 g, 1.0 mmol) in hot ethanol (3 mL). Blue powder precipitated immediately. The resulting solid was filtered off, dried under reduced pressure, and used for the further reactions.

Synthesis of [Ph4P]₂[Co(N₃)₄]·0.5H₂O (1). An excess of NaN₃ (0.50 g, 7.7 mmol) was slowly added to a solution of [Ph₄P]₂[CoCl₄] (0.25 g, 0.28 mmol) in acetone (10 mL). The mixture was allowed to stir overnight at room temperature. Then it was filtered and concentrated to 5 mL. The vapour of absolute ether was diffused into the concentrated filtrate to give diffraction quality blue crystals of 1 in 78% yield. Anal. Calc. (%) for C₄₈H₄₁CoN₁₂O_{0.5}P₂: C, 63.02; H, 4.52; N, 18.37. Found: C, 63.16; H, 4.78; N, 18.20%. IR (cm⁻¹): 3347 (w), 3080 (w), 2048 (s), 1721 (w), 1655 (w), 1585 (w), 1483 (w), 1435 (m), 1345 (w), 1108 (s), 995 (w), 758 (w), 723 (s), 691 (m), 527 (s).

Synthesis of [Ph4P]₂[Co(NCO)₄] (2). Blue crystals of **2** were prepared by a procedure similar to that in the preparation of **1**, except the same equivalent KNCO instead of NaN₃ was used. Yield 74%. Anal. Calc. (%) for C₅₂H₄₀CoN₄P₂O₄: C, 68.95; H, 4.45; N, 6.19. Found: C, 69.00; H, 4.50; N, 6.19%. IR (cm⁻¹): 3130 (m), 2207 (s), 1680 (w), 1584 (w), 1482 (m), 1438 (s), 1401 (s), 1320 (m), 1186(w), 1107 (s), 996 (w), 758 (w), 723 (s), 690 (m), 613 (m), 526 (s).

Synthesis of [Ph4P]2[Co(NCS)4] (3). Blue crystals of **3** were prepared by a procedure similar to that in the preparation of **1**, but using the same equivalent KNCS instead of NaN₃. Yield 77%. Anal. Calc. (%) for C₅₂H₄₀CoN₄P₂S₄: C, 64.38; H, 4.16; N, 5.78. Found: C, 64.38; H, 4.15; N, 5.74%. IR (cm⁻¹): 3131 (m), 2079 (s), 1678 (w), 1582 (w), 1480 (w), 1436 (m), 1400 (s), 1316 (w), 1186(w), 1105 (s), 995 (w), 753 (w), 722 (s), 688 (m), 527 (s), 474 (w).

X-ray single-crystal structure determinations

Single crystal X-ray diffraction data were collected on a Bruker SMART APEX II diffractometer with a CCD area detector (Mo- K_{α} radiation, $\lambda = 0.71073$ Å) at 296 K. The APEX II program was used to determine the lattice parameters and for data collection. The data were integrated and corrected using SAINT.¹⁹ The absorption corrections were applied using the 'multi-scan' method with SADABS.²⁰ The structures were solved by the direct methods and refined on F² by full-matrix least squares using SHELXTL-97.²¹ All non-hydrogen atoms were refined with anisotropic thermal parameters, and all hydrogen atoms were located at calculated positions and generated by the riding model.

Magnetic measurements

Magnetic measurements were performed on polycrystalline samples restrained in a frozen eicosane matrix using a Quantum Design SQUID VSM magnetometer. Direct-current (dc) magnetic data were recorded at fields up to 7 T in the range of

Journal Name ARTICLE

1.8-300 K. Alternating-current (ac) susceptibility measurements were carried out under an oscillating ac field of 0.2 mT and ac frequencies ranging from 1 to 1000 Hz. Direct-current magnetic susceptibilities were corrected for diamagnetism using Pascal constants²² and a sample holder correction.

Results and discussion

Structural features

Single-crystal X-ray diffraction analyses show that **1-3** crystallize in the monoclinic $P2_1/n$ or C2/c space group (Table S3) with $[Co(E)_4]^{2^-}$ ($E = N_3^-$, **1**; $E = NCO^-$, **2**; NCS^- , **3**) anion and Ph_4P^+ cations. A crystalline water molecule is found in **1**. The structures of the anions are depicted in Fig. 1. Selected bond lengths and bond angles are given in Table 1. The CoN4 anion can be described as a distorted tetrahedron. The structure of $[Co(NCS)_4]^{2^-}$ has been reported in some cases, $^{10e-10h,23}$ while only three structures containing $[Co(NCO)_4]^{2^-}$ and one containing $[Co(N3)_4]^{2^-}$ are known, all with different cations than Ph_4P^+ in the current work.

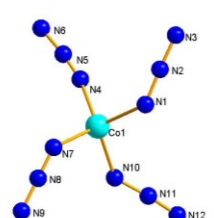


Table 1 Selected bond lengths (Å) and angles (°) for 1-3

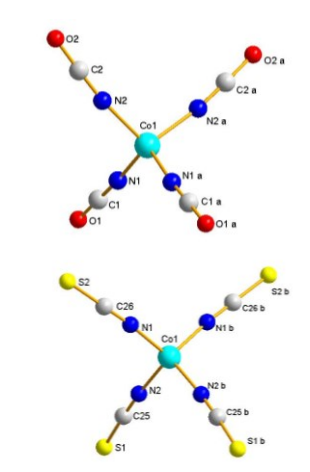


Fig. 1 Molecular structures of the anions of 1-3.

In 1, the Co-N bond lengths are in the range of 1.910(11)-1.984(10) Å with an average value of 1.942 Å, which is shorter than those in 2 (1.956(2)-1.976(3) Å) and 3 (1.943(2)-1.949(3) Å). These Co-N bond length differences could be due to the coordination abilities of these three pseudohalides

| 1 | 1 | | | 3 | |
|-------------------|-----------|------------------------|------------|----------------------------|------------|
| Bond length: | s | Bond len | gths | Bond leng | gths |
| Co(1)-N(1) | 1.938(11) | Co(1)-N(1) | 1.956(2) | Co(1)-N(1) | 1.943(2) |
| Co(1)-N(4) | 1.910(11) | $Co(1)-N(1)^a$ | 1.956(2) | Co(1)-N(1)b | 1.943(2) |
| Co(1)-N(7) | 1.934(10) | Co(1)-N(2) | 1.976(3) | Co(1)-N(2) | 1.949(3) |
| Co(1)-N(10) | 1.984(10) | $Co(1)-N(2)^a$ | 1.976(3) | Co(1)-N(2)b | 1.949(3) |
| Bond angles | 3 | Bond ang | gles | Bond ang | gles |
| N(1)-Co-N(4) | 106.6(5) | $N(1)$ -Co- $N(1)^a$ | 115.28(15) | $N(1)$ -Co- $N(1)^b$ | 112.13(15) |
| N(1)-Co-N(7) | 105.9(4) | $N(1)^a$ -Co- $N(2)^a$ | 108.79(11) | $N(1)$ -Co- $N(2)^b$ | 109.63(11) |
| N(1)-Co-N(10) | 112.9(4) | $N(1)$ -Co- $N(2)^a$ | 108.91(11) | $N(1)^{b}$ -Co- $N(2)^{b}$ | 110.24(11) |
| N(4)-Co-N(7) | 116.1(5) | $N(1)^a$ -Co-N(2) | 108.91(11) | N(1)-Co-N(2) | 110.24(11) |
| N(4)-Co-N(10) | 109.7(5) | N(1)-Co-N(2) | 108.79(11) | $N(1)^b$ -Co-N(2) | 109.63(11) |
| N(7)-Co-N(10) | 105.7(4) | $N(2)$ -Co- $N(2)^a$ | 105.74(17) | $N(2)$ -Co- $N(2)^b$ | 104.72(16) |
| N(1)-N(2)-N(3) | 176.4(12) | N(1)-C(1)-O(1) | 178.7(3) | N(2)-C(25)-S(1) | 177.6(2) |
| N(4)-N(5)-N(6) | 174.1(17) | N(2)-C(2)-O(2) | 178.3(3) | N(1)-C(26)-S(2) | 179.8(3) |
| N(7)-N(8)-N(9) | 178.8(12) | Co-N(1)-C(1) | 176.2(3) | Co-N(1)-C(26) | 172.3(3) |
| N(10)-N(11)-N(12) | 173.1(11) | Co-N(2)-C(2) | 172.0(3) | Co-N(2)-C(25) | 174.8(2) |
| Co-N(1)-N(2) | 125.4(8) | | | | |
| Co-N(4)-N(5) | 156.2(14) | | | | |
| Co-N(7)-N(8) | 133.8(9) | | | | |
| Co-N(10)-N(11) | 133.6(8) | | | | |

Symmetry codes: (a) -x+1, y, -z+3/2; (b) -x+1, y, -z+3/2

The N-Co-N bond angles varies from 105.7(4) to $116.1(5)^\circ$ in **1**, 105.74(17) to $115.28(15)^\circ$ in **2** and 104.72(16) to $112.13(15)^\circ$ in **3**. These Co-N bond lengths and N-Co-N bond

angles are similar to those of other reported tetra (pseudohalide)-cobalt(II) complexes. $^{10e\text{-}10h,23,24}$

The most marked difference between 1 and 2-3 is the bond angles Co-N-X. The Co-N-N angles in 1 are significantly bent in

125.4(8), 133.6(8), 133.8(9), and 156.2(14)°, while the Co-N-C angles are 172.0(3) and 176.2(3)° in **2** and 172.3(3) and 174.8(2)° in **3**. However, the N₃-, NCO- and NCS- ligands remain linear with 173.1(11), 174.1(17), 176.4(12) and 178.1(12)° in **1**, 178.7(3) and 178.3(3)° in **2**, 177.6(2) and 179.8(3)° in **3**. All the Co-N-X, N-N-N, N-C-O and N-C-S angles in **1-3** are close to those of the reported earlier with different cations. 10f,10h,23,24

In order to further evaluate the degree of distortion of the Co^{2+} center in 1-3 from the ideal T_d symmetry, continuous shape measurement analyses were performed using the SHAPE 2.1 program. The calculated value provides an estimate of the distortion from the ideal structure with 0 corresponds to the ideal polyhedron. The calculated values relative to the ideal tetrahedron geometry are 0.223, 0.073 and 0.055 for 1-3, respectively (Table S4). These small values suggest the small deviations from the ideal tetrahedron. Obviously, the distortion of 1 is the largest among the three complexes.

The Co(II) ions are well-separated with the shortest Co···Co distance of 10.22 Å, 7.51 Å and 8.12 Å for 1-3, respectively, thus precluding any prominent intermolecular magnetic interactions.

Static magnetic properties

Direct-current (dc) magnetic characterization of 1-3 were performed at 2.0-300 K under an applied dc field of 0.1 T. The temperature dependence of the molar magnetic susceptibility $(\chi_{\rm M})$ per Co(II) ion presented in the form of $\chi_{\rm M}T$ vs T plots are shown in Fig. 2a and Fig. S4-S7. The $\chi_M T$ values of 2.53, 2.46, and 2.33 cm³·K·mol⁻¹ at 300 K for 1-3, respectively, are consistent with an S = 3/2 spin center with g value of 2.32, 2.29, and 2.23. Each $\chi_{\rm M}T$ product is significantly larger than the spinonly value of one isolated high spin Co(II) ion (1.875 cm³·K·mol⁻¹ with S = 3/2, g = 2.0) and falls within the reported range of 2.1-3.4 cm³·K·mol⁻¹. These results are consistent with a single non-interacting Co(II) ion with a considerable orbital angular momentum contribution.²⁶ When the temperature is lowered, the $\chi_{\rm M}T$ product remains nearly constant to 90 (1), 30 (2), and 25 K (3) and then significantly decreases to a minimum value of 1.64, 1.77, and 1.74 cm³·K·mol⁻¹ at 2.0 K, respectively. Such a turndown in low temperature range is mainly due to the intrinsic magnetic anisotropy of the Co(II) ion in 1-3, rather than intermolecular interactions because of the intermolecular distances between the Co(II) ions.

To further investigate the static magnetic behavior, field-dependent magnetizations were measured for **1-3** under applied magnetic fields in the range of 1-7 T at 1.8 K, which are presented in Fig. S8. The magnetizations at 7 T are 2.38, 3.11, and 3.15 $N_{A}\mu_{B}$, respectively, for **1-3**, which have not reached the saturation, another sign for the strong magnetic anisotropy. Moreover, the non-superposition of M vs B/T curves at various applied dc fields and 1.8-5.0 K (Fig. 2b and Fig. S4-S7) further indicate the presence of considerable magnetic anisotropies in **1-3**.

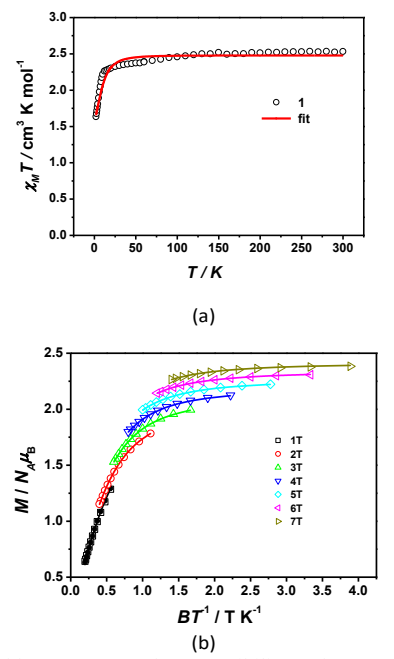


Fig. 2 (a) Variable-temperature dc susceptibility under an applied dc field of 0.1 T for 1. (b) Variable-temperature, variable-field dc magnetization data of 1. Fields of 1-7 T were used at temperatures from 1.8 K to 5.0 K. Solid lines are the best fits with PHI program.²⁷

To further investigate the static magnetic behavior, field-dependent magnetizations were measured for **1-3** under applied magnetic fields in the range of 1-7 T at 1.8 K, which are presented in Fig. S8. The magnetizations at 7 T are 2.38, 3.11, and 3.15 $N_{A}\mu_{B}$, respectively, for **1-3**, which have not reached the saturation, another sign for the strong magnetic anisotropy. Moreover, the non-superposition of M vs B/T curves at various applied dc fields and 1.8-5.0 K (Fig. 2b and Fig. S4-S7) further indicate the presence of considerable magnetic anisotropies in **1-3**.

To estimate the ZFS parameters D and E, representing magnetic anisotropies of **1-3**, the $\chi_{\rm M}T$ vs T and M vs B/T curves were simultaneously analyzed by using PHI program, 27 with the spin Hamiltonian as given in Eqn (1):

$$\hat{H} = D(\hat{S}_z^2 - S(S+1)/3) + E(\hat{S}_x^2 - \hat{S}_y^2) + \mu_B g \hat{S} B$$
 (1)

in which μ_B denotes the Bohr magneton, D, E, S and B represent the axial and rhombic ZFS parameters, spin, and magnetic field vector, respectively. The parameters from the best fitting results are summarized in Table 2. Although dc magnetic data usually cannot yield accurate magnitude and sign of D and E parameters, reasonable results for $\mathbf{1}$ were obtained only when the sign of D was assigned to be negative. However, both reasonable fits can be obtained for $\mathbf{2}$ and $\mathbf{3}$ with both positive and negative D values. Therefore, it is impossible to confirm the nature of D parameter sorely based on the dc magnetic data (Fig. S4-S7). From the fitting parameters in Table 2, the magnitude of D value of D is larger than those of D and D0, probably due to the high degree of structural distortion in D1, which is consistent with the larger distortion values of D1 calculated by the continuous shape measurement analyses.

Journal Name ARTICLE

Table 2 The fitting parameters from the direct-current magnetic data for 1-3

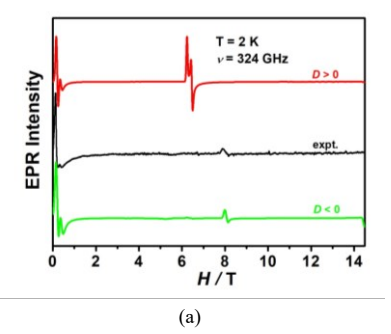
| | D, cm ⁻¹ | E, cm ⁻¹ | $g_{x,y}$ | $g_{\rm z}$ |
|---|---------------------|---------------------|-----------|-------------|
| 1 | -12.09(3) | 1.74(5) | 2.275(2) | 2.342(1) |
| 2 | 4.89(9) | 0.01(3) | 2.266(3) | 2.330(6) |
| | -4.93(1) | 0.03(3) | 2.265(2) | 2.324(2) |
| 3 | 3.79(1) | 0.13(7) | 2.246(1) | 2.188(2) |
| | -3.53(6) | 0.13(7) | 2.247(3) | 2.184(4) |

HFEPR Studies

HFEPR spectroscopy²⁸ was used to further study the nature of magnetic anisotropies of **1-3**. The HFEPR spectra were recorded for the powder samples of **1-3** with different frequencies and magnetic fields (Fig. S9 and Fig. 3-4). As shown in Fig. S9, there is no obvious HFEPR signal found for **1**. However, there are several resonance signals observed for **2** and **3** at 2 K under different frequencies.

In a high-spin Co(II) system, there are two types of possible EPR transitions, i.e. intra-Kramers and inter-Kramers EPR transitions. When the $Ms=\pm 3/2$ Kramers doublet lies at lower energy than the $Ms=\pm 1/2$ doublet, corresponding to easy-axis magnetic anisotropy, the intra-Kramers EPR transition within the $\pm 3/2$ doublet corresponding to $\Delta Ms=\pm 3$ is nominally forbidden. This transition could be partly allowed when a sizable rhombic ZFS E term mixes the $\pm 3/2$ doublet with the $\pm 1/2$ doublet. However the transition between the $Ms=\pm 3/2$ Kramers doublet and the $Ms=\pm 1/2$ doublet is possible when the energy separation is smaller than the microwave energy in the HFEPR. The absence of HFEPR signal in 1 suggests that the magnetic anisotropy is easy-axial and $2(D^2+3E^2)^{1/2}$ are larger than the frequency range in our measurements (~13 cm⁻¹).

In the HFEPR spectrum of **2** at 324 GHz (Fig. 3), a resonance near zero field is observed, giving a roughly estimated value of $2(D^2 + 3E^2)^{1/2}$ as 10.8 cm^{-1} . Then $D = 5.4 \text{ cm}^{-1}$ and E = 0 were used as the initial values for the simulations. The two-dimensional curve of resonance fields at various used frequencies was established and showed in Fig. 3b, where the transitions are plotted as squares. The curve was simulated by spin Hamiltonian (Eqn 1) with program Spin.²⁹ The derived spin Hamiltonian parameters are $D = -5.23 \text{ cm}^{-1}$, $E = 0.056 \text{ cm}^{-1}$, $g_{xy} = 2.2$, and $g_z = 2.18$. If the sign of D was assigned as positive, no reasonably simulated spectra was obtained (Fig. 3a), confirming the negative sign of D in **2**. In comparison, the absence of HFEPR transitions in **1** suggest that of the D parameter of **1** is also negative but the magnitude is larger than that in **2**.



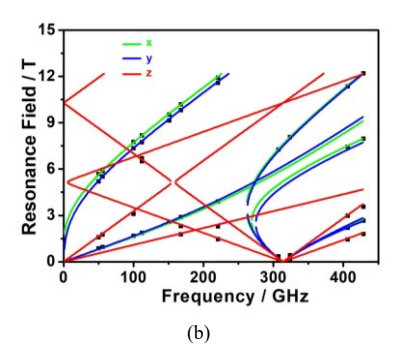
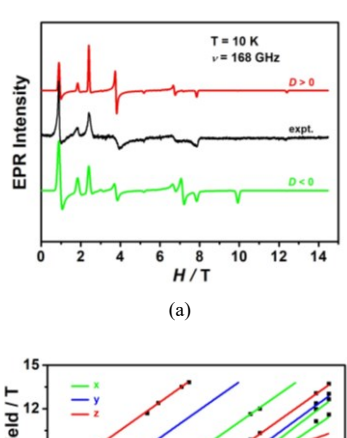


Fig. 3 (a) HFEPR spectrum of 2 at 2 K (black) and its simulations (red trace: positive D; green trace: negative D) at 324 GHz; (b) Resonance field vs microwave frequency (quantum energy) for EPR transitions for **2**. Simulations were conducted by program Spin. ²⁹ Solid lines show the (x, y, z) transitions as labeled.



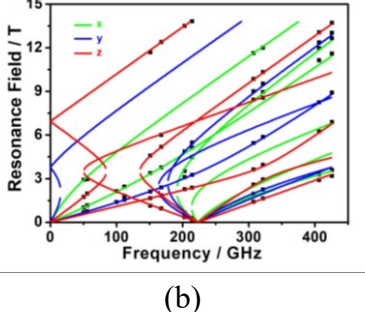


Fig. 4 (a) HFEPR spectrum of 3 at 10 K (black) and its simulations (red trace: positive D; green trace: negative D) at 168 GHz; (b) Resonance field vs microwave frequency (quantum energy) for EPR transitions for $\bf 3$. Simulations were conducted by program Spin.29 Solid lines show the (x, y, z) transitions as labeled.

For complex 3, a typical EPR spectrum at 10 K with 168 GHz is shown in Fig. 4a. A 2D map of resonance fields at various microwave frequencies was plotted in Fig. 4b and was simulated by spin Hamiltonian (Eqn 1) with program Spin.²⁹ The derived

spin Hamiltonian parameters are D = +3.63 cm⁻¹, E = 0.49 cm⁻¹, $g_{xy} = 2.27$, $g_z = 2.22$. The sign of D value was determined to be positive by the comparison between the experimental spectrum at 168 GHz and the simulated one with both the negative and positive D values (Fig. 4b).

To conclude, HFEPR spectra showed the easy-axis anisotropy for $\bf 1$ and $\bf 2$ but easy-plane anisotropy for $\bf 3$. The larger magnitude of D in $\bf 1$ prevented its exact determination, but a negative sign was deduced.

Theoretical studies of magnetic anisotropies in 1-3

In order to get further insight into magnetic anisotropies in 1-3 varying with the different pseudo-halides, ab initio calculations were performed for the experimentally determined structures of 1-3 using Molcas 8.2 program package.³⁰ Calculation details are given in ESI.

The calculated energies of the spin-free states and spin-orbit states are listed in Tables S5-S6. The first excited spin-free state is in the range of 3370.6-4468.1 cm⁻¹ above the ground one for **1-3**, suggesting that the lowest quartet term is well isolated from the excited ones. The energy differences between the lowest two spin-free states (Table S5) of **1-3** are much larger than those between the lowest two spin-orbit states (Table S6). The ground spin-orbit state for **1-3** are almost composed of the ground spin-free one. These are consistent with the orbital nondegeneracy of the ground term in **1-3**, which allow us to use spin Hamiltonian (Eqn 1) with the ZFS parameters D and E to model their magnetic anisotropies. The calculated ZFS parameters D(E) (cm⁻¹) and g (g_x , g_y , g_z) tensors of **1-3** are listed in Table S7. The calculated D(E) values of -7.1(0.93), -3.4(-0.05) and 2.0(0.03) cm⁻¹ are comparable with those determined by HFEPR.

The calculated $\chi_{\rm M}T$ versus T plots of **1-3** are shown in Fig. S11. The calculated $g_{\rm x}$, $g_{\rm y}$, $g_{\rm z}$ orientations of the ground spin-orbit states on Co(II) ions of **1-3** are shown in Fig. S12.

Dynamic magnetic properties

The ac susceptibility measurements were performed for 1-3 with the aim to study the dynamic magnetic behaviors at the low temperatures. No out-of-phase ac susceptibility (χ_M ") signal was observed under zero applied dc field at 1.8 K (Fig. S13), which could be due to the occurrence of quantum tunneling of the magnetization (QTM). A small dc field would efficiently suppress the QTM and induce nonzero χ_M " signals. It was found that the $\chi_{\rm M}$ " signal intensified as the applied dc field increases for 1. A peak of χ_M " appears at 0.02 T and shifts to low frequencies and then remains nearly constant at the same frequency. The peak reaches the maximum at 0.08 T. Similarly, a maximum of $\chi_{\rm M}$ " of 2 is found with an applied field of 0.02 T, which shifts to low frequencies and the moving speed becomes quite slow after 0.10 T, but the maximum value of χ_M " decreases sharply. In contrast, no maximum of χ_M " is observed for 3, but the intensities of χ_M " signals gradually enhances with the increasing of the applied magnetic field. Magnetic field of 0.08 T for 1, 0.10 T for 2 and 3 were then chosen for further temperature- and frequencydependent ac measurements at 1.8-5.0 K (Fig. 5-7). Temperature-dependent xm" signals were observed below 2.6 K (1), 4.0 K (2) and 4.5 K (3) as shown in the χ_{M} " vs T plots (Fig. S14-S16). These data confirm that 1-3 exhibit field-induced slow magnetic relaxation.

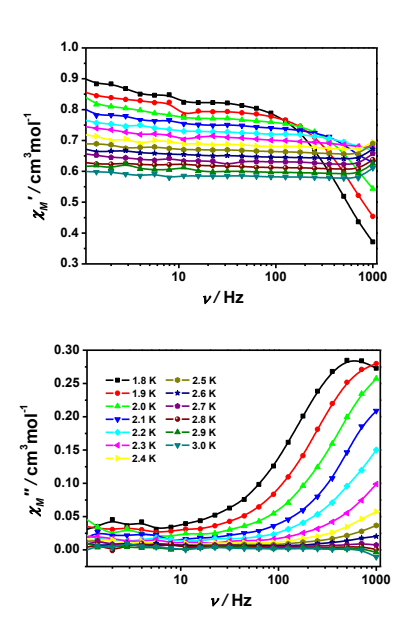


Fig. 5 Frequency dependence of in-phase (χ_M') and out-of-phase (χ_M'') ac magnetic susceptibilities from 1.8 to 3.0 K under 0.08 T dc field for 1. The solid lines are for eye guide.

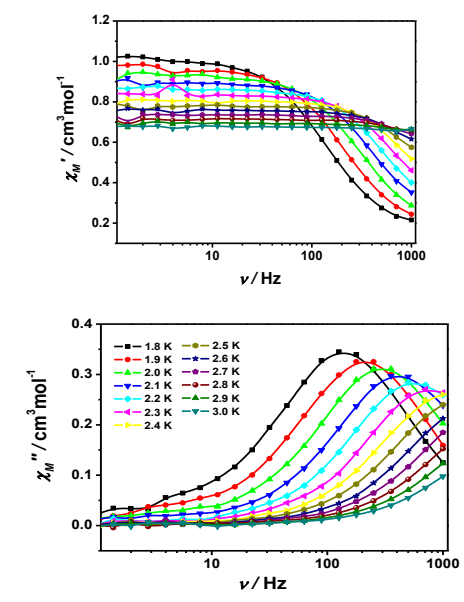


Fig. 6 Frequency dependence of in-phase (χ_M') and out-of-phase (χ_M'') ac magnetic susceptibilities from 1.8 to 3.0 K under 0.10 T dc field for **2**. The solid lines are for eye guide.

Journal Name ARTICLE

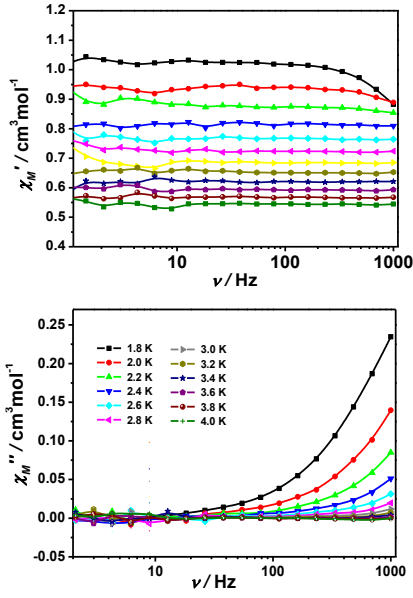


Fig. 7 Frequency dependence of in-phase (χ_M') and out-of-phase (χ_M'') ac magnetic susceptibilities from 1.8 to 4.0 K under 0.1 T dc field for 3. The solid lines are for eye guide.

To determine the relaxation times at different temperatures, the Cole-Cole plots for **2** were constructed in the range of 1.8-2.6 K (Fig. S17) which were fitted with the generalized Debye model by Eqn (2):³¹

$$\chi_{ac}(\omega) = \chi_S + \frac{\chi_T - \chi_S}{1 + (i\omega\tau)^{(1-\alpha)}}$$
 (2)

The fitting parameters of χ_T (isothermal susceptibility), χ_S (adiabatic susceptibility), τ (relaxation time) and α (deviation from a pure Debye model) are summarized in Table S8. The resulting parameters α are in the range of 0.09-0.13 for 2, indicating that the distribution of relaxation times are very small and only one relaxation process is present.

If a SIM supposedly has only one characteristic time, corresponding to a Debye relaxation process with one activation energy ($U_{\rm eff}$), the relaxation time (τ) may be written in terms of the Arrhenius law $\tau = \tau_0 \exp(U_{\rm eff}/k_{\rm B}T)$. The τ values of **2** extracted from the Debye model were fit to give $U_{\rm eff} = 10.5 \, {\rm cm}^{-1}$ and $\tau_0 = 3.63 \times 10^{-7} \, {\rm s}$ (Fig. S18). The effective energy barrier of **2** is consistent with the $2(D^2+3E^2)^{1/2}$ value ($10.8 \, {\rm cm}^{-1}$) expected for an Orbach process.

For 1 and 3, because of only one or no χ_M " peak was observed (Fig. 5 and 7), which prevents to further analysis to the relaxation processes. It can be concluded that the relaxation in 1 and 3 is much faster than 2.

Conclusions

In this paper, we present the synthesis, structures and magnetic properties of three mononuclear tetrakis(pseudohalido)-cobalt(II) complexes $(Ph_4P)_2[Co(N_3)_4]\cdot 0.5H_2O$ (1) and $(Ph_4P)_2[Co(E)_4]$ (E = NCO⁻, 2; NCS⁻, 3). The structural determinations show that the central anionic moiety CoN₄ in 1-3

is a distorted tetrahedron. The detailed dc magnetic measurements and HFEPR suggested the sensitivity of the magnetic anisotropy varying with the nature of the ligands. Easy-axis magnetic anisotropy was found for 1 and 2 but easy-plane anisotropy for 3, which is supported by the ab initio calculations. According to the ac susceptibilities, the three complexes exhibit slow magnetic relaxation under an applied field and thus are field-induced SIMs. The current work adds three new numbers to mononuclear tetrahedral Co(II) SIMs family.

Conflicts of interest

There are no conflicts to declare.

Acknowledgements

We are grateful for the financial support from the Natural Science Grant of China (No. 21471078 to XTC), and the US National Science Foundation (CHE-1900296 to ZLX).

Notes and references

- (a) D. Gatteschi, R. Sessoli and J. Villain, Molecular Nanomagnets, Oxford University Press, Oxford, UK, 2006;
 (b) P. C. E. Stamp and A. Gaita-Arino, J. Mater. Chem., 2009, 19, 1718;
 (c) W. Wernsdorfer and R. Sessoli, Science, 1999, 284, 133;
 (d) M. N. Leuenberger and D. Loss, Nature, 2001, 410, 789.
- R. Sessoli, H. L. Tsai, A. R. Schake, S. Wang, J. B. Vincent, K. Folting, D. Gatteschi, R. Sessoli, G. Christou and D. N. Hendrickson, *J. Am. Chem. Soc.*, 1993, 115, 1804.
- 3 F. Neese, D. A. Pantazis, Faraday Discuss. 2011, 148, 229.
- 4 D. N. Woodruff, R. E. P. Winpenny and R. A. Layfield, *Chem. Rev.*, 2013, **113**, 5110.
- (a) M. Feng and M.-L. Tong, Chem. Eur. J. 2018, 24, 7574;
 (b) G. A. Craig and M. Murrie, Chem. Soc. Rev., 2015, 44, 2135;
 (c) A. K. Bar, C. Pichon and J.-P. Sutter, Coord. Chem. Rev., 2016, 308, 346;
 (d) J. M. Frost, K. L. M. Harriman and M. Murugesu, Chem. Sci., 2016, 7, 2470;
 (e) A. Sarkar, S. Dey, and G. Rajaraman, Chem. Eur. J. 2020, 26, 14036.
- 6 P. C. Bunting, M. Atanasov, E. Damgaard-Møller, M. Perfetti, I. Crassee, M. Orlita, J. Overgaard, J. V. Slageren, F. Neese and J. R. Long, *Science*, 2018, 362, 1.
- 7 F. Deng, T. Han, B. Yin and Y.-Z. Zheng, *Inorg. Chem. Front.*, 2017, 4, 1141.
- (a) S. Ziegenbalg, D. Hornig, H. Görls, W. Plass, , *Inorg. Chem.* 2016, 55, 4047; (b) S. Vaidya, A. Upadhyay, S. K. Singh, T. Gupta, S. Tewary, S. K. Langley, J. P. S. Walsh, K. S. Murray, G. Rajaraman and M. Shanmugam, *Chem. Commun.*, 2015, 51, 3739; (c) L. Smolko, J. Černák, M. Dušek, J. Miklovič, J. Titiš and R. Boča, *Dalton Trans.*, 2015, 44, 17565; (d) L. Smolko, J. Černák, M. Dušek, J. Titiš and R. Boča, *New J. Chem.*, 2016, 40, 6593; (e) L. Smolko, J. Černák, J. Kuchár, C. Rajnák, J. Titiš and R. Boča, *Eur. J. Inorg. Chem.*, 2017, 24, 3086; (f) A. Switlicka, B. Machura, R. Kruszynski, J. Cano, L. M. Toma, F. Lloret and M. Julve, *Dalton Trans.*, 2018, 47, 5831; (g) S. Vaidya, P. Shukla, S. Tripathi, E. Rivière, T. Mallah, G. Rajaraman and M. Shanmugam, Inorg. Chem., 2018, 57, 3371.
- (a) J. M. Zadrozny and J. R. Long, J. Am. Chem. Soc., 2011,
 133, 20732; (b) J. M. Zadrozny, J. Telser and J. R. Long,
 Polyhedron, 2013, 64, 209; (c) E. A. Suturina, J. Nehrkorn,

- J. M. Zadrozny, J. Liu, M. Atanasov, T. Weyhermüller, D. Maganas, S. Hill, A. Schnegg, E. Bill, J. R. Long and F. Neese, Inorg. Chem., 2017, 56, 3102; (d) M. S. Fataftah, J. M. Zadrozny, D. M. Rogers and D. E. Freedman, Inorg. Chem., 2014, 53, 10716; (e) M. S. Fataftah, S. C. Coste, B. Vlaisavljevich, J. M. Zadrozny and D. E. Freedman, Chem. Sci., 2016, 7, 6160; (f) S. Vaidya, S. Tewary, S. K. Singh, S. K. Langley, K. S. Murray, Y. Lan, W. Wernsdorfer, G. Rajaraman and M. Shanmugam, Inorg. Chem., 2016, 55, 9564; (g) S. Sottini, G. Poneti, S. Ciattini, N. Levesanos, E. Ferentinos, J. Krzystek, L. Sorace and P. Kyritsis, *Inorg.* Chem., 2016, 55, 9537; (h) D. Tu, D. Shao, H. Yan and C. Lu, Chem. Commun., 2016, 52, 14326; (i) D. R. Alcoba, O. B. Oña, G. E. Massaccesi, A. Torre, L. Lain, J. I. Melo, J. E. Peralta and J. M. Oliva-Enrich, Inorg. Chem., 2018, 57, 7763; (j) K. Chattopadhyay, M. J. H. Ojea, A. Sarkar, M. Murrie, G. Rajaraman and D. Ray, Inorg. Chem., 2018, 57, 13176; (k) X.-N. Yao, M.-W. Yang, J. Xiong, J.-J. Liu, C. Gao, Y.-S. Meng, S.-D. Jiang, B.-W. Wang and S. Gao, Inorg. Chem. Front., 2017, 4, 701.
- (a) Y. Rechkemmer, F. D. Breitgoff, M. van der Meer, M. Atanasov, M. Hakl, M. Orlita, P. Neugebauer, F. Neese, B. Sarkar and J. van Slageren, *Nature Commun.*, 2016, 7, 1; (b) E. Carl, S. Demeshko, F. Meyer and D. Stalke, Chem. Eur. J., 2015, 21, 10109; (c) J. Vallejo, E. Pardo, M. Viciano-Chumillas, I. Castro, P. Amorós, M. Déniz, C. Ruiz-Pérez, C. Yuste-Vivas, J. Krzystek, M. Julve, F. Lloreta and J. Cano, Chem. Sci., 2017, 8, 3694; (d) R. Bruno, J. Vallejo, N. Marino, G. D. Munno, J. Krzystek, J. Cano, E. Pardo and D. Armentano, *Inorg. Chem.*, 2017, **56**, 1857; (e) Y.-Y. Zhu, F. Liu, J.-J. Liu, Y.-S. Meng, S.-D. Jiang, A.-L. Barra, W. Wernsdorfer and S. Gao, *Inorg. Chem.*, 2017, **56**, 697; (f) L. H. G. Kalinke, J. C. O. Cardoso, R. Rabelo, A. K. Valdo, F. T. Martins, J. Cano, M. Julve, F. Lloret and D. Cangussu. Eur. J. Inorg. Chem., 2018, 816; (g) D. Shao, L.-D. Deng, L. Shi, D.-Q. Wu, X.-Q. Wei, S.-R. Yang, and X.-Y. Wang, Eur. J. Inorg. Chem., 2017, 3862; (h) J. Palion-Gazda, B. Machura, R. Kruszynski, T. Grancha, N. Moliner, F. Lloret, and M. Julve, Inorg. Chem., 2017, 56, 6281.
- 11 (a) A. Piecha-Bisiorek, A. Bieńko, R. Jakubas, R. Boča, M. Weselski, V. Kinzhybalo, A. Pietraszko, M. Wojciechowska, W. Medycki and D. Kruk, J. Phys. Chem. A, 2016, 120, 2014; (b) O. Y. Vassilyeva, E. A. Buvaylo, V. N. Kokozay, B. W. Skelton, C. Rajnák, J. Titiš and R. Boča, Dalton Trans., 2019, 48, 11278.
- T. Jurca, A. Farghal, P.-H. Lin, I. Korobkov, M. Murugesu and D. S. richeson, J. Am. Chem. Soc., 2011, 133, 15814;
 (b) D. Schweinfurth, M. G. Sommer, M. Atanasov, S. Demeshko, S. Hohloch, F. Meyer, F. Neese and B. Sarkar, J. Am. Chem. Soc., 2015, 137, 1993.
- 13 J. Vallejo, I. Castro, R. Ruiz-García, J. Cano, M. Julve, F. Lloret, G. De Munno, W. Wernsdorfer and E. Pardo, *J. Am. Chem. Soc.*, 2012, **134**, 15704.
- 14 X.-C. Huang, C. Zhou, D. Shao and X.-Y. Wang, *Inorg. Chem.*, 2014, 53, 12671.
- L. Chen, J. Wang, J.-M. Wei, W. Wernsdorfer, X.-T. Chen, Y.-Q. Zhang, Y. Song and Z.-L. Xue, *J. Am. Chem. Soc.*, 2014, 136, 12213.
- 16 J. Krzystek, D. C. Swenson, S. A. Zvyagin, D. Smirnov, A. Ozarowski and J. Telser, J. Am. Chem. Soc., 2010, 132, 5241.
- 17 (a) S. L. Wang, L. Li, Z. W. Ouyang, Z. C. Xia, N. M. Xia, T. Peng and K. B. Zhang, *Acta Phys. Sin.*, 2012, **61**, 107601(1–5); (b) H. Nojiri and Z. W. Ouyang, *Terahertz Sci. Technol.*, 2012, **5**, 1.
- 18 E. Styczeń, Z. Warnke and D. Wyrzykowski, *Thermochim. Acta*, 2007, **454**, 84.

- 19 SAINT Software Users Guide, Version 7.0, Bruker Analytical X-ray Systems, Madison, 1999.
- G. M. Sheldrick, SADABS, Version 2.03, Bruker Analytical X-ray Systems, Madison, 2000.
- 21 G. M. Sheldrick, Acta Crystallogr. A, 2008, **64**, 112.
- 22 G. A. Bain and J. F. Berry, *J. Chem. Educ.*, 2008, **85**, 532.
- 23 S. S. Massoud, M. Dubin, A. E. Guilbeau, M. Spell, R. Vicente, P. Wilfling, R. C. Fischer and F. A. Mautner, *Polyhedron*, 2014, 78, 135.
- 24 (a) K. Ruhlandt-Senge, I. Sens and U. Müller, Z. Naturforsch., 1991, 46b, 1689; (b) A. Ray, G. M. Rosair, R. Kadam and S. Mitra, Polyhedron, 2009, 28, 796.
- (a) M. Llunell, D. Casanova, J. Cirera, P. Alemany and S. Alvarez, *Shape Program*, Version 2.1, 2013; (b) S. Alvarez, P. Alemany, D. Casanova, J. Cirera, M. Llunell and D. Avnir, *Coord. Chem. Rev.*, 2005, 249, 1693.
- 26 F. E. Mabbs and D. J. Machin, Magnetism and Transition Matal Complexes, Dover Publications: Mineola, NY, 2008.
- 27 N. F. Chilton, R. P. Anderson, L. D. Turner, A. Soncini and K. S. Murray, *J. Comput. Chem.*, 2013, **34**, 1164.
- 28 (a) J. Krzystek, O. Ozarowski and J. Telser, Coord. Chem. Rev., 2006, 250, 2308; (b) J. Krzystek, S. A. Zvyagin, O. Ozarowski, S. Trofimenko and J. Telser, J. Magn. Reson., 2006, 178, 174.
- 29 Simulations were performed using SPIN developed by Andrew Ozarowski at the National High Magnetic Field Laboratory, USA.
- 30 F. Aquilante, J. Autschbach, R. K. Carlson, L. F. Chibotaru, M. G. Delcey, L. De Vico, I. Fdez. Galván, N. Ferré, L. M. Frutos, L. Gagliardi, M. Garavelli, A. Giussani, C. E. Hoyer, G. Li Manni, H. Lischka, D. Ma, P. Å. Malmqvist, T. Müller, A. Nenov, M. Olivucci, T. B. Pedersen, D. Peng, F. Plasser, B. Pritchard, M. Reiher, I. Rivalta, I. Schapiro, J. Segarra-Martí, M. Stenrup, D. G. Truhlar, L. Ungur, A. Valentini, S. Vancoillie, V. Veryazov, V. P. Vysotskiy, O. Weingart, F. Zapata and R. Lindh, J. Comput. Chem., 2016, 37, 506.
- 31 (a) Y.-N. Guo, G.-F. Xu, Y. Guo and J. Tang, *Dalton Trans.*, 2011, **40**, 9953; (b) K. S. Cole and R. H. Cole, *J. Chem. Phys.*, 1941, **9**, 341.

Magnetic anisotropies and slow magnetic relaxation of three tetrahedral tetrakis(pseudohalido)-cobalt(II) complexes

Shu-Yang Chen,^a Wei Lv,^a Hui-Hui Cui,^a Yi-Quan Zhang,^{b*} Xue-Tai Chen,^{a*} Zhenxing Wang,^{c*} Zhong-Wen Ouyang,^c Lei Chen,^d Hong Yan,^{a*} Zi-Ling Xue^e

aState Key Laboratory of Coordination Chemistry, School of Chemistry and Chemical Engineering, Nanjing University, Nanjing 210023, China. E-mail: xtchen@nju.edu.cn; hyan1965@nju.edu.cn

^bSchool of Environmental and Chemical Engineering, Jiangsu University of Science and Technology, Zhenjiang 212003, China.

^cJiangsu Key Laboratory for NSLSCS, School of Physical Science and Technology, Nanjing Normal University, Nanjing 210023, China. Email: zhangyiquan@njnu.edu.cn
^dWuhan National High Magnetic Field Center & School of Physics, Huazhong University of Science and Technology, Wuhan 430074, China. Email: zxwang@hust.edu.cn
^eDepartment of Chemistry, University of Tennessee, Knoxville, Tennessee 37996, USA.

Electronic Supplementary Information

Table S1 Four-coordinate Co(II)-SIMs with the four identical donors

| complexes | coodination | D (cm ⁻¹) | $U_{\it eff}$ (cm ⁻¹) | H _{dc} (kOe) | Ref. |
|--|-------------------|-----------------------|-----------------------------------|-----------------------|------|
| (Ph ₄ P) ₂ [Co(OPh) ₄](CH ₃ CN) | CoO ₄ | -11.1 | 21 | 1.4 | S1 |
| K(Ph ₄ P)[Co(OPh) ₄] | CoO ₄ | -23.8 | - | 0 | S1 |
| $[\text{Co}^{\text{II}}\text{Co}^{\text{III}}_4\text{L}^1_2(\mu_{1,3}\text{-O}_2\text{CCH}_3)_2(\mu\text{-OH})_2](\text{ClO}_4)_2\cdot 4\text{H}_2\text{O}$ | CoO ₄ | -31.31 | - | 3.0 | S2 |
| $[\text{Co}^{\text{II}}\text{Co}^{\text{III}}_4\text{L}^1_2(\mu_{1,3}\text{-O}_2\text{CC}_2\text{H}_5)_2(\mu\text{-OH})(\mu\text{-OMe})](\text{ClO}_4)_4\cdot 5\text{H}_2\text{O}$ | CoO ₄ | -21.88 | - | 3.0 | S2 |
| $[\text{Co}^{\text{II}}\text{Co}^{\text{III}}_4\text{L}^2_2(\mu_{1,3}\text{-O}_2\text{CCH}_3)_2(\mu\text{-OH})_2](\text{ClO}_4)_4\cdot\text{H}_2\text{O}$ | CoO ₄ | -23.6 | 20.9 | 1.0 | S3 |
| $[\text{Co}^{\text{II}}\text{Co}^{\text{III}}_4\text{L}^2_2(\mu_{1,3}\text{-O}_2\text{CC}_2\text{H}_5)_2(\mu\text{-OH})_2](\text{ClO}_4)_4\cdot\text{H}_2\text{O}$ | CoO ₄ | -24.3 | 22.9 | 1.0 | S3 |
| $(Ph_4P)_2[Co(SPh)_4]$ | CoS ₄ | -70 | 21 | 0 | S4 |
| $(Ph_4P)_2[Co(SPh)_4]$ | CoS ₄ | -62 | 21 | 0 | S1 |
| (K(18C6)) ₂ [Co(C ₃ S ₅) ₂] | CoS ₄ | -166 | 91 | 0 | S5 |
| $(Ph_4P)_2[Co(C_3S_5)_2]$ | CoS ₄ | -161 | 33.9 | 0 | S6 |
| $(Bu_4N)_2[Co(C_3S_5)_2]$ | CoS ₄ | -113.7 | - | 0 | S7 |
| $(Ph_4P)_2[Co(C_3S_5)_2]$ | CoS ₄ | -116.4 | - | 0 | S7 |
| (PPN) ₂ [Co(C ₃ S ₅) ₂] | CoS ₄ | -105.7 | - | 0 | S7 |
| $(K(18C6))_2[Co(C_3S_5)_2]$ | CoS ₄ | -118.0 | 91 | 0 | S7 |
| (HNEt3)2[Co(L3)2] | CoS ₄ | -71.6 | 26.8 | 1.0 | S8 |
| $[Co(L^4)_4](NO_3)_2$ | CoS ₄ | -61.7 | 19.5 | 0 | S9 |
| $[\operatorname{Co}(\operatorname{L}^5)_4](\operatorname{ClO}_4)_2$ | CoS ₄ | -80.7 | 32.7 | 0 | S9 |
| $[\operatorname{Co}(\operatorname{L}^6)_4](\operatorname{ClO}_4)_2$ | CoS ₄ | -70.8 | 18.7 | 2.0 | S9 |
| $[\operatorname{Co}(L^7)_4](\operatorname{ClO}_4)_2$ | CoS ₄ | -21.3 | 13.2 | 2.0 | S9 |
| $[\text{Co}(^{i}\text{Pr}_{2}\text{PSNPS}^{i}\text{Pr}_{2})_{2}]$ | CoS ₄ | -30.5 | 49 | 1.0 | S10 |
| $Co[(SPPh_2)_2N]_2$ | CoS ₄ | -11.8 | 25.3 | 1.0 | S11 |
| [Co(NH ₂ CSNH ₂) ₄](SiF ₆) | CoS ₄ | -5.1 | 34.8 | 0 | S12 |
| $(Ph_4P)_2[Co(SePh)_4]$ | CoSe ₄ | -83 | 19 | 0 | S1 |

| [Co(ⁱ Pr ₂ PSeNPSe ⁱ Pr ₂) ₂] | CoSe ₄ | -30.4 | - | 1.0 | S14 |
|---|-------------------|--------|------|-----|-----|
| $Co[(SePPh_2)_2N]_2$ | CoSe ₄ | -15.8 | 29.2 | 1.0 | S15 |
| $Co[(TePiPr_2)_2N]_2$ | CoTe ₄ | -45.1 | 22 | 0 | S15 |
| (HNEt ₃) ₂ [Co(dmps) ₂] | CoN ₄ | -115 | 118 | 0 | S13 |
| (TTF) ₂ [Co(pdms) ₂] | CoN ₄ | -112 | 24.1 | 0 | S14 |
| $[Co((NtBu)_3SMe)_2]$ | CoN ₄ | -58 | 75 | 0 | S15 |
| [Co(dmbpy) ₂](ClO ₄) ₂ | CoN ₄ | -57 | 73.9 | 2.5 | S16 |
| $(Bu_4N)_2[Co(L^8)_2]\cdot H_2O$ | CoN ₄ | -130.8 | 58.4 | 0 | S17 |
| $(HNEt_3)_2[Co(L^9)_2]\!\cdot\!H_2O$ | CoN ₄ | -144.1 | 46.0 | 0 | S17 |
| $K_2[Co(bmsab)_2]$ | CoN ₄ | -118 | - | 0 | S18 |
| (K-18-c-6) ₂ [Co(bmsab) ₂] | CoN ₄ | -130 | - | 0 | S18 |
| $(HNEt_3)_2[Co(btsab)_2]$ | CoN ₄ | -110 | - | 0 | S18 |
| [Co(cytosine) ₂ (NCS) ₂] | CoN ₄ | -6.1 | 13.0 | 1.0 | S19 |
| [Co(cytosine) ₂ (NCO) ₂] | CoN ₄ | -7.4 | 19.1 | 1.0 | S19 |
| [CoL ¹⁰ ₂](ClO ₄) ₂ | CoN ₄ | -45.9 | 46.9 | 1.0 | S20 |
| $[K(C_{12}H_{24}O_6)][Co(NCS)_4]$ | CoN ₄ | +2.7 | - | 0.5 | S21 |
| $[Ba(C_{12}H_{24}O_6)\cdot 3H_2O][Co(NCS)_4]$ | CoN ₄ | +5.2 | - | 2.0 | S21 |
| (C ₃ N ₂ H ₅) ₂ [CoCl ₄] | CoCl ₄ | -12.0 | - | 3.0 | S22 |
| $(C_{13}N_3H_{12})_2[CoCl_4]$ | CoCl ₄ | 12.1 | - | 4.0 | S23 |

 $H_3L^1=2,6$ -bis((2-(2-hydroxyethylamino)-ethylimino)methyl)-4-methylphenol; $H_3L^2=(2,6$ -bis- [{2-(2-hydroxyethylthio)ethylimino}methyl]-4-methylphenol; $H_2L^3=1,2$ -dithiol-o-carborane; $L^4=$ thiourea; $L^5=1,3$ -n-butylthiourea; $L^6=1,3$ -phenylethylthiourea; $L^7=1,1,3,3$ -tetramethylthiourea; $H_2pdms=1,2$ -bis(methanesulfonamido) benzene; dmbpy = 6,6'-dimethyl-2,2'-bipyridine; $H_2L^8=N,N'$ -diphenyloxamide; $H_2L^9=N,N'$ -bis(p-toluenesulfonyl) oxamide; TTF = tetrathiafulvalene; bmsab = 1,2-bis(methanesulfonamido)benzene; btsab = 1,2-bis-(toluenesulfonamido)benzene; $L^{10}=2,9$ -diphenyl-1,10-phenanthroline.

Table S2 Summary of the magnetic properties of [Co(NCX)₄]²⁻ complexes with diamagnetic or spin-crossover cations

| complex | D (cm ⁻¹) | E (cm ⁻¹) | SIM^d | Ref. |
|--|-----------------------|-----------------------|---------|------|
| [K(C ₁₂ H ₂₄ O ₆)] ₂ [Co(NCS) ₄] | $+2.57^{a}$ | 0.82^{a} | Yes | S24 |
| $[Ba(C_{12}H_{24}O_6)\cdot 3H_2O][Co(NCS)_4]$ | +5.56 ^a | 1.05^{a} | Yes | S24 |
| HgCo(NCS) ₄ | +5.39 a | 0 | Yes | S25 |
| [Ni(Me6trans[14]dieneN4)][Co(NCS) ₄] | $+3.74^{b}$ | 0.051^{b} | no | S26 |
| [Ni(Me6trans[14]dieneN4)] ₂ [Co(NCS) ₄](ClO ₄) ₂ ·H ₂ O | +11.6 ^b | 0.023^{b} | Yes | S26 |
| [Ni(Me6trans[14]dieneN4)] ₂ [Co(NCS) ₄](PF ₆) ₂ | $+7.29^{b}$ | 0.50^{b} | Yes | S26 |
| $[Co(tppz)_2][Co(NCS)_4]\cdot MeOH$ | $+3.8^{b}$ | 0^c | No | S27 |
| $[Co(Brphterpy)_2][Co(NCS)_4] \cdot 2MeCN$ | $+7.55^{b}$ | 0.01^{b} | Yes | S28 |
| $[Co(tppz)_2][Co(NCO)_4] \cdot 2H_2O$ | +4.3 ^b | 0^c | Yes | S27 |

Note: a. D and E determined by HFEPR spectra; b. D and E values estimated by magnetic data; c. These E value was assumed to be zero; d. "Yes" and "No" mean if the slow magnetic relaxation is observed or not by the conventional SQUID.

Adding the formula/names for the ligands as in Table S1?

Table S3 Crystal Data and Structure Refinement for 1-3

| | 1 | 2 | 3 |
|---|---|--|--|
| empirical formula | C ₄₈ H ₄₁ CoN ₁₂ O _{0.5} P ₂ | C ₅₂ H ₄₀ CoN ₄ P ₂ O ₄ | C ₅₂ H ₄₀ CoN ₄ P ₂ S ₄ |
| formula weight, g•mol ⁻¹ | 914.80 | 905.75 | 969.99 |
| <i>T</i> , K | 296(2) | 296(2) | 296(2) |
| crystal system | monoclinic | monoclinic | monoclinic |
| space group | $P2_1/n$ | C2/c | C2/c |
| a, Å | 14.3325(8) | 22.276(3) | 22.538(3) |
| b, Å | 21.246(2) | 14.828(3) | 15.0939(18) |
| c, Å | 15.7637(17) | 13.6901(18) | 14.9601(18) |
| β , deg | 95.24(2) | 104.641(4) | 108.721(2) |
| V, Å ³ | 4780.2(8) | 4375.1(11) | 4820.0(10) |
| Z | 4 | 4 | 4 |
| D _c , g•cm ⁻³ | 1.270 | 1.375 | 1.337 |
| F(000) | 1892 | 1876 | 2004 |
| absorption coefficient,mm ⁻¹ | 0.473 | 0.518 | 0.636 |
| crystal size, mm | $0.19 \times 0.15 \times 0.12$ | $0.22 \times 0.20 \times 0.16$ | $0.22 \times 0.16 \times 0.14$ |
| θ range for data collection | 1.72 - 19.66 | 2.10 - 27.52 | 1.65 - 27.49 |
| | $-13 \le h \le 13$ | $-28 \le h \le 26$ | $-29 \le h \le 25$ |
| Index ranges | $-20 \le k \le 19$ | $-19 \le k \le 15$ | $-8 \le k \le 19$ |
| | $-14 \le l \le 14$ | $-15 \le l \le 17$ | $-18 \le l \le 19$ |
| reflection collected | 19743 | 18416 | 11628 |
| independent reflections | $4184 \ (R_{\rm int} = 0.0608)$ | $5037 (R_{\rm int} = 0.0793)$ | $5419 (R_{\rm int} = 0.0279)$ |
| data/restraints/parameters | 4184/0/580 | 5037/0/285 | 5419/0/285 |
| completeness | 0.987 | 0.999 | 0.977 |
| goodness-of-fit on F^2 | 1.162 | 1.098 | 1.092 |
| | $R_1 = 0.0643$, | $R_1 = 0.0570,$ | $R_1 = 0.0515,$ |
| final <i>R</i> indices $[I \ge 2\sigma(I)]$ | $wR_2 = 0.1664$ | $wR_2 = 0.1205$ | $wR_2 = 0.1251$ |
| | $R_1 = 0.0855,$ | $R_1 = 0.0757,$ | $R_1 = 0.0691,$ |
| R indices (all data) | $wR_2 = 0.1825$ | $wR_2 = 0.1269$ | $wR_2 = 0.1384$ |
| largest diff. peak and hole | 0.694 and -0.398 | 0.683 and -0.409 | 0.501 and -0.814 |
| CCDC No. | 2024569 | 1945219 | 1945220 |

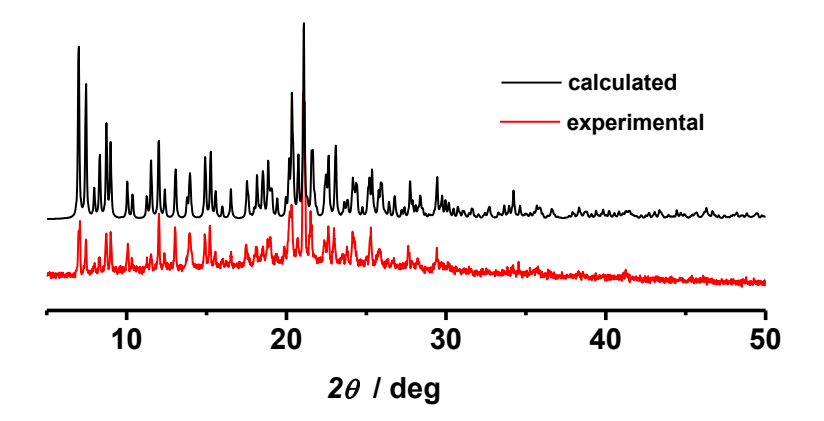


Fig. S1 XRD patterns for complex 1.

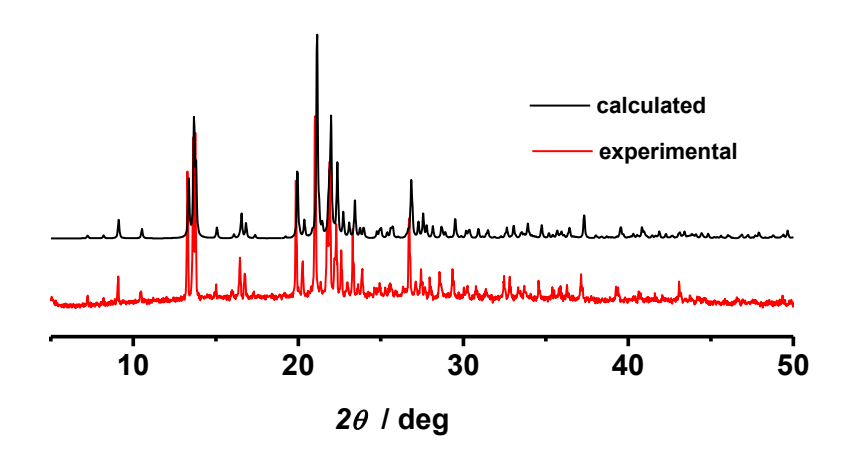


Fig. S2 XRD patterns for complex 2.

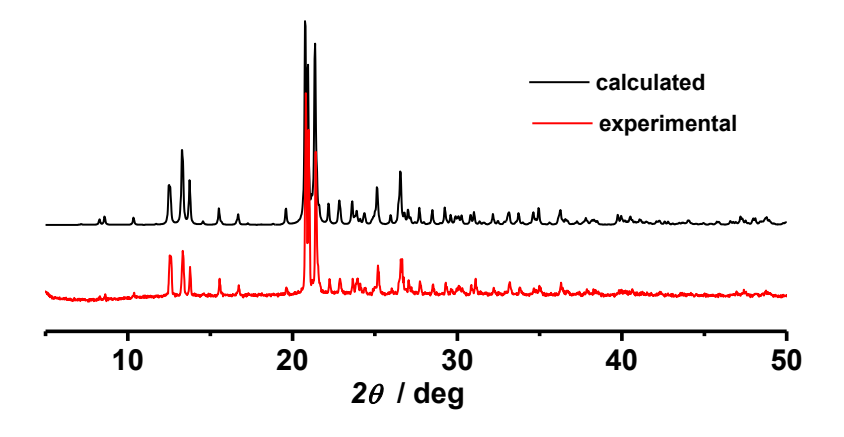


Fig. S3 XRD patterns for complex 3.

Table S4 The results of the continuous shape measure analyses of anions in 1-3 by the SHAPE software. S29

| | 1 | 2 | 3 |
|--------------------------------------|--------|--------|--------|
| Square (D _{4h}) | 29.315 | 32.548 | 32.672 |
| Tetrahedron (T_d) | 0.223 | 0.073 | 0.055 |
| Seesaw (C_{2v}) | 7.988 | 8.393 | 9.322 |
| Vacant trigonal bipyramid (C_{3v}) | 3.391 | 3.095 | 3.170 |

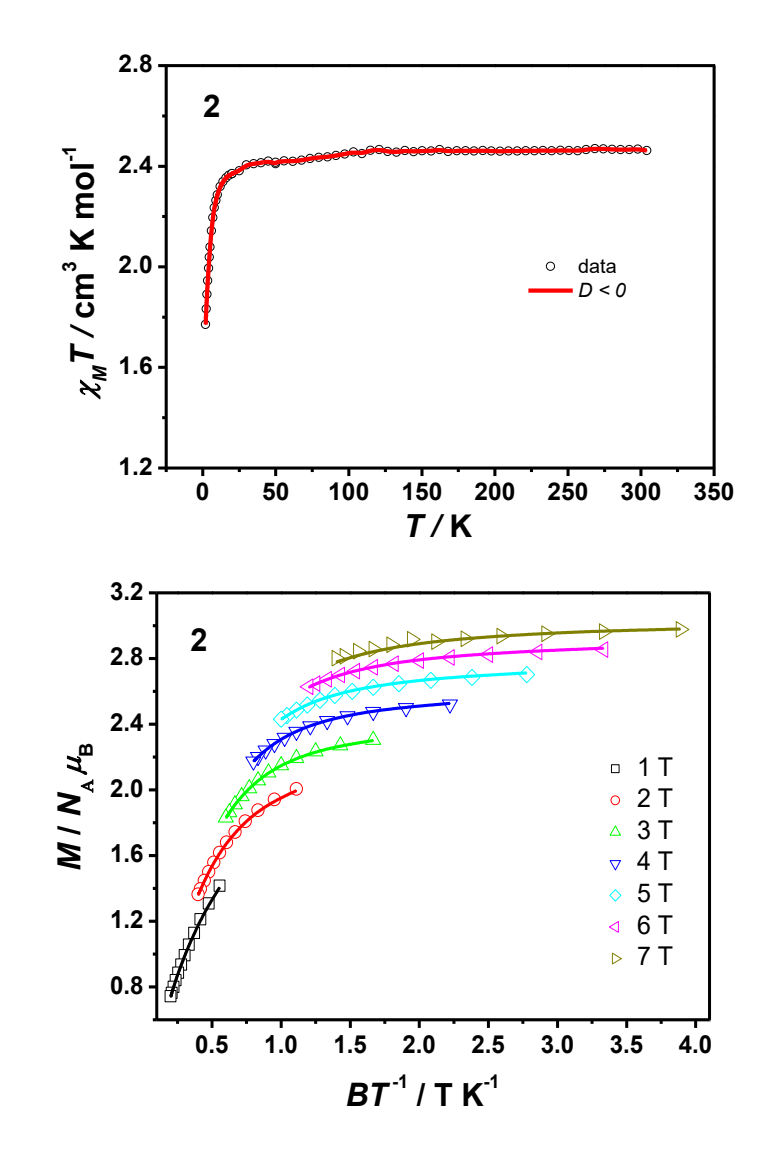


Fig. S4 Variable-temperature dc susceptibilities and variable- temperature, variable -field dc magnetization data of **2**. Fields of 1-7 T were used at temperatures from 1.8 K to 5.0 K. Solid lines are the fits with the *PHI* program when the *D* value was assigned as negative.

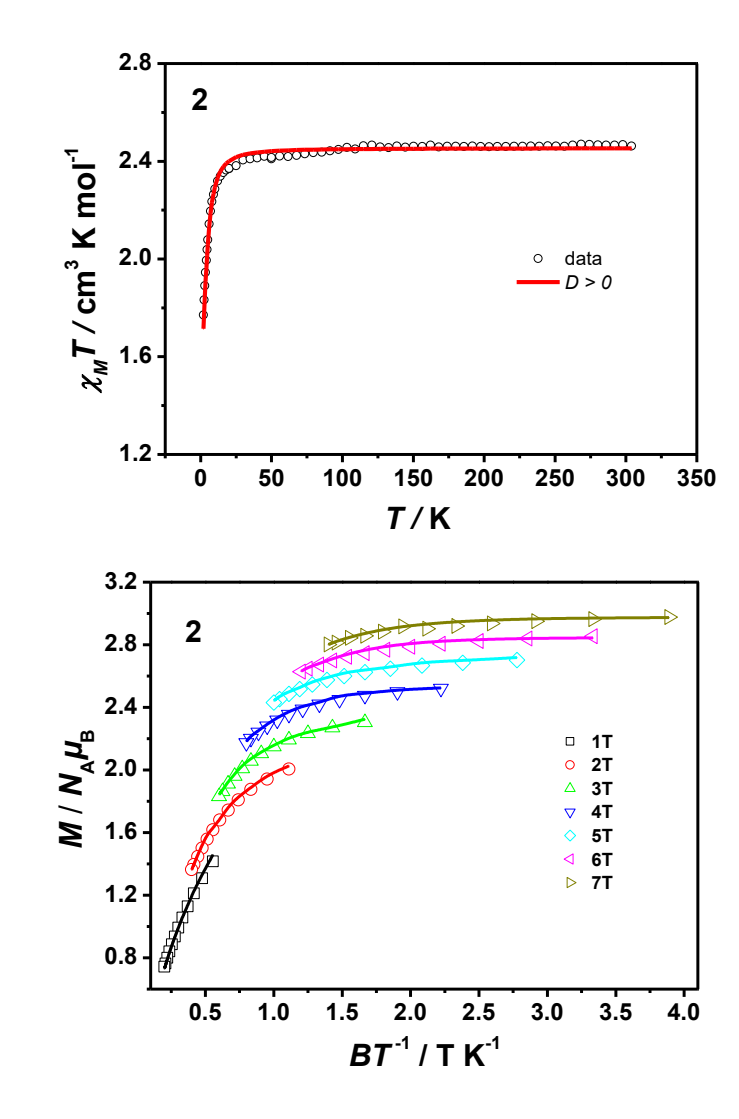


Fig. S5 Variable-temperature dc susceptibilities and variable- temperature, variable -field dc magnetization data of **2**. Fields of 1-7 T were used at temperatures from 1.8 K to 5.0 K. Solid lines are the fits with the *PHI* program when the *D* value was assigned as positive.

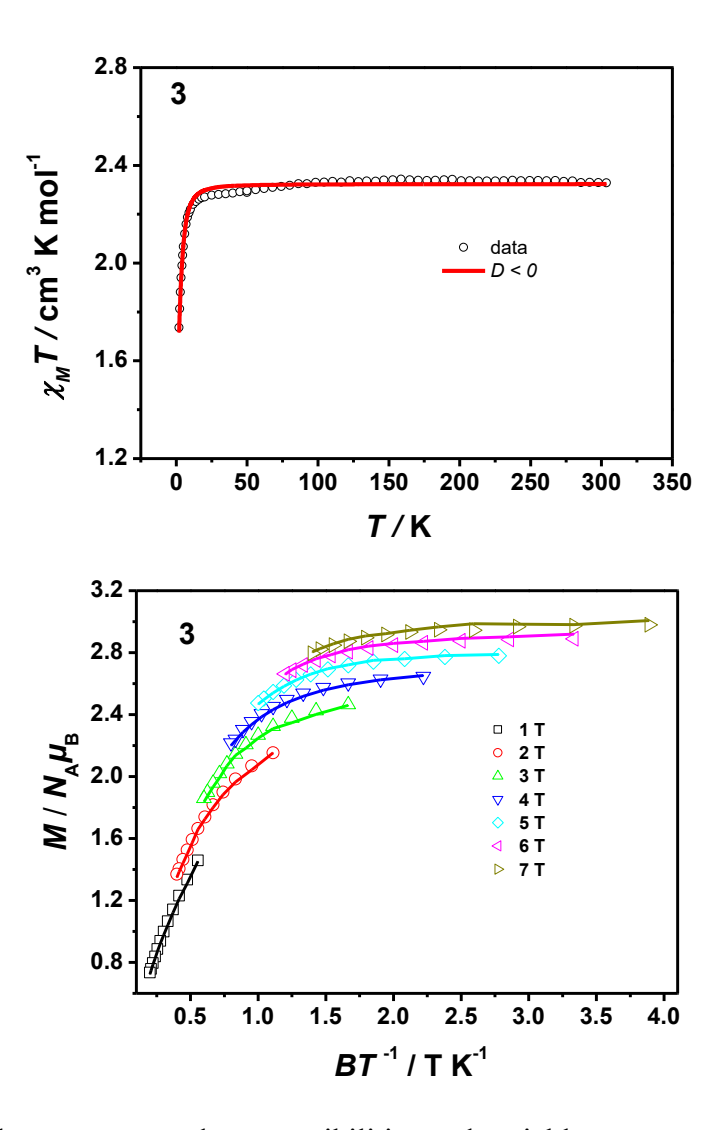


Fig. S6 Variable-temperature dc susceptibilities and variable- temperature, variable -field dc magnetization data of **3**. Fields of 1-7 T were used at temperatures from 1.8 K to 5.0 K. Solid lines indicate the fits with the *PHI* program when the *D* value was assigned as negative.

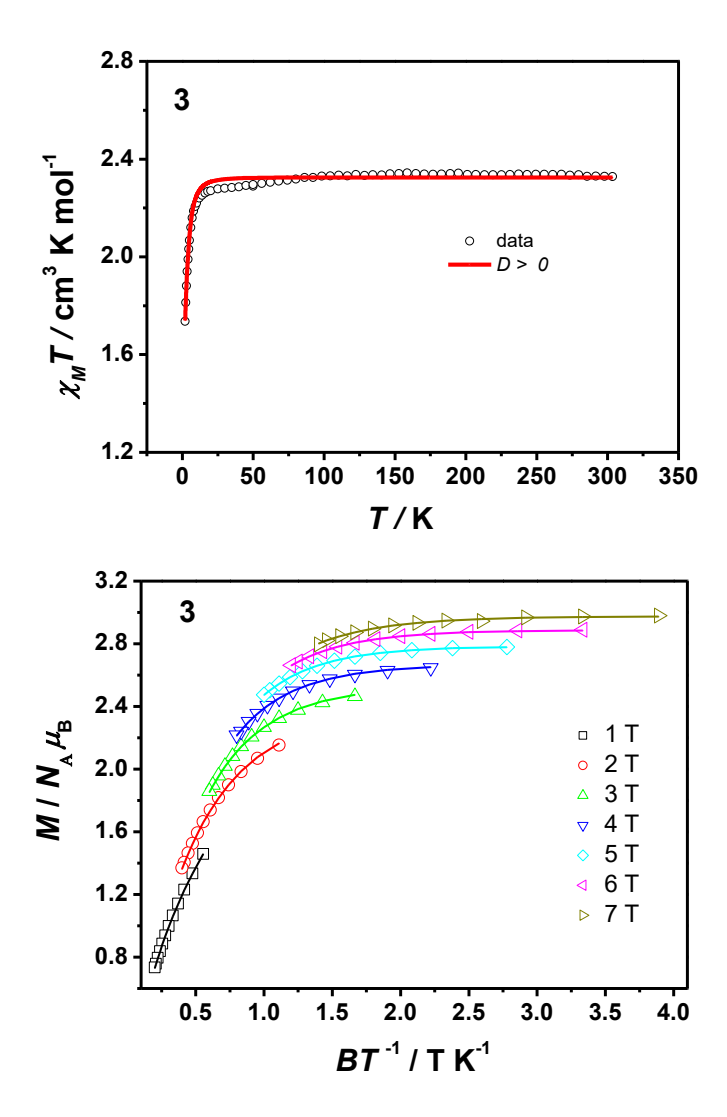


Fig. S7 Variable-temperature dc susceptibilities and variable- temperature, variable -field dc magnetization data of **3**. Fields of 1-7 T were used at temperatures from 1.8 K to 5.0 K. Solid lines indicate the fits with the *PHI* program when the *D* value was assigned as positive.

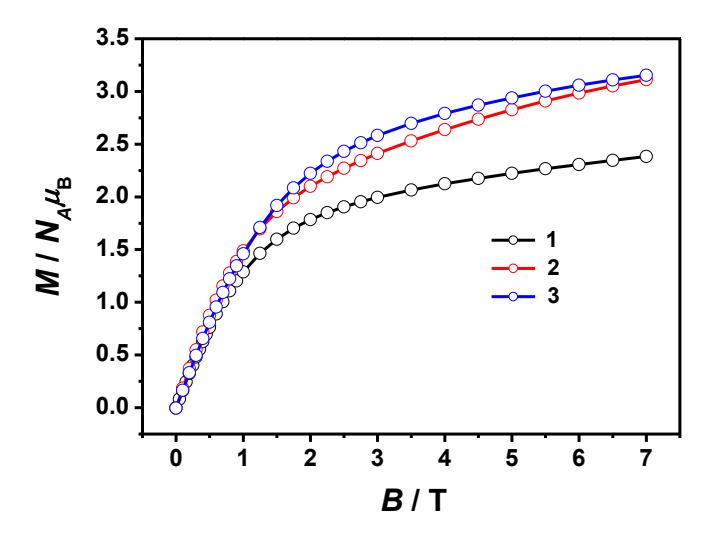


Fig. S8 The isothermal field dependence of magnetization at 1.8 K for 1-3.

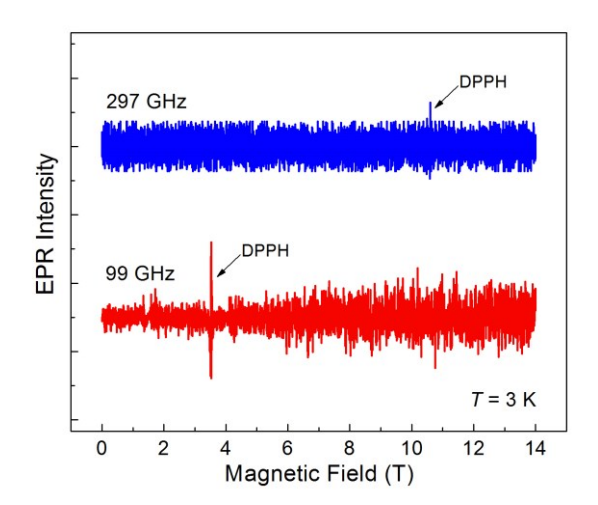


Fig. S9 The experimental HFEPR spectra in derivative mode for **1** under 99 and 297 GHz at 3 K.

Ab initio calculation

Complete-active-space self-consistent field (CASSCF) calculations with MOLCAS 8.2^{S31} program package were performed on **1–3** (see Fig. S9 for the calculated complete structures of **1–3**) on the basis of X-ray determined geometries.

The basis sets for all atoms are atomic natural orbitals from the MOLCAS ANO-RCC library: ANO-RCC-VTZP for Co(II) ion; VTZ for close N ions; VDZ for distant atoms. The calculations employed the second order Douglas-Kroll-Hess Hamiltonian, where scalar relativistic contractions were taken into account in the basis set. And then, the spin-orbit couplings were handled separately in the restricted active space state interaction (RASSI-SO) procedure. The active electrons in 10 active spaces considering the 3*d*-double shell effect (5+5') include all seven 3*d* electrons (CAS(7 in 5+5') for Co(II)), and the mixed spin-free states are 50 (all from 10 quadruplets and all from 40 doublets for Co(II)). SINGLE_ANISO^{S32-S34} program was used to obtain the spin-free energies, spin-orbit energies, parameters *D(E)* (cm⁻¹), *g* tensors, magnetic axes, *et al.*, based on the above CASSCF/RASSI-SO calculations.

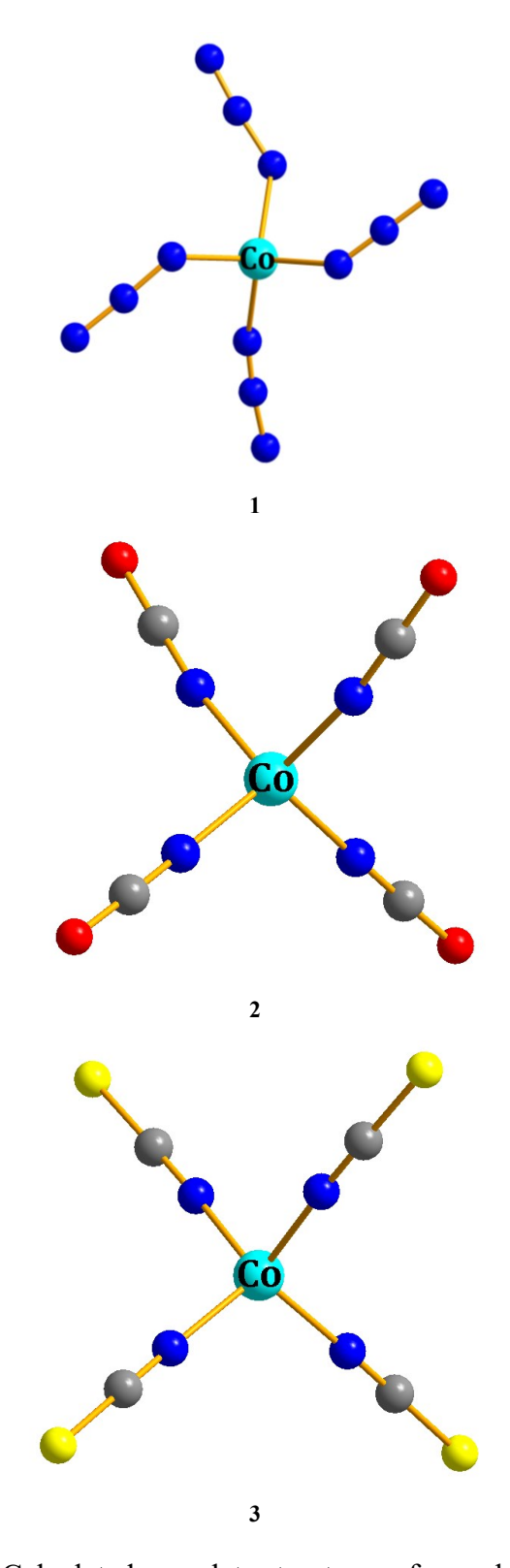


Fig. \$10 Calculated complete structures of complexes 1-3.

Table S5. Calculated spin-free energies (cm⁻¹) of the lowest ten terms (S = 3/2) of complexes **1-3** using CASSCF/ RASSI-SO with MOLCAS 8.2.

| | 1 | 2 | 3 |
|----|----------------------|----------------------|----------------------|
| | E/cm^{-1} | E/cm^{-1} | E/cm^{-1} |
| 1 | 0.0 | 0.0 | 0.0 |
| 2 | 3370.6 | 4057.6 | 4468.1 |
| 3 | 4184.3 | 4098.4 | 4627.4 |
| 4 | 4566.7 | 4370.7 | 4724.1 |
| 5 | 6479.0 | 6975.7 | 7603.0 |
| 6 | 7247.4 | 7177.8 | 8036.4 |
| 7 | 7367.2 | 7624.2 | 8311.1 |
| 8 | 20442.4 | 20864.6 | 21492.6 |
| 9 | 20877.6 | 21355.4 | 21563.1 |
| 10 | 21378.3 | 21500.6 | 21918.6 |

Table S6 Calculated weights of the five most important spin-orbit-free states for the lowest two spin-orbit states of **1-3** using CASSCF/RASSI-SO with MOLCAS 8.2.

| | Spin-orbit | Energy | | Spin-free states, Spin, Weights | | | | |
|---|------------|---------------------|---------------|---------------------------------|------------------|---------------|---------------|--|
| | states | (cm ⁻¹) | | 3piii-1 | ree states, 5pm, | Weights | | |
| 1 | 1 | 0.0 | 1,1.5,0.9713 | 2,1.5,0.0191 | 3,1.5,0.0049 | 4,1.5,0.0033 | 18,0.5,0.0005 | |
| 1 | 2 | 14.5 | 1,1.5,0.9779 | 3,1.5,0.0091 | 4,1.5,0.0089 | 2,1.5,0.0028 | 17,0.5,0.0006 | |
| | 1 | 0.0 | 1,1.5,0.9759 | 2,1.5,0.0119 | 3,1.5,0.0068 | 4,1.5,0.0041 | 17,0.5,0.0005 | |
| 2 | 2 | 6.9 | 1,1.5, 0.9775 | 4,1.5,0.0093 | 3,1.5,0.0080 | 2,1.5,0.0040 | 18,0.5,0.0006 | |
| , | 1 | 0.0 | 1,1.5,0.9803 | 2,1.5,0.0089 | 4,1.5,0.0077 | 3,1.5, 0.0020 | 17,0.5,0.0007 | |
| 3 | 2 | 4.0 | 1,1.5,0.9810 | 3,1.5,0.0096 | 4,1.5,0.0043 | 2,1.5,0.0040 | 18,0.5,0.0005 | |

Table S7. Calculated zero-field splitting parameters D (E) (cm⁻¹) and g (g_x , g_y , g_z) tensors of the lowest spin-orbit states of complexes 1-3 using CASSCF/RASSI-SO with MOLCAS 8.2.

| | 2 | | 3 | |
|-------|--------------------------|----------------------------|--------------------------|----------------|
| g | D(E) (cm ⁻¹) | g | D(E) (cm ⁻¹) | g |
| 2.249 | | 2.268 | | 2.264 |
| 2.269 | -3.4(-0.05) | 2.271 | 2.0(0.03) | 2.261 |
| 2.348 | | 2.306 | | 2.242 |
| | 2.249 2.269 | 2.249 2.269 -3.4(-0.05) | 2.249 2.269 | 2.249 2.269 |

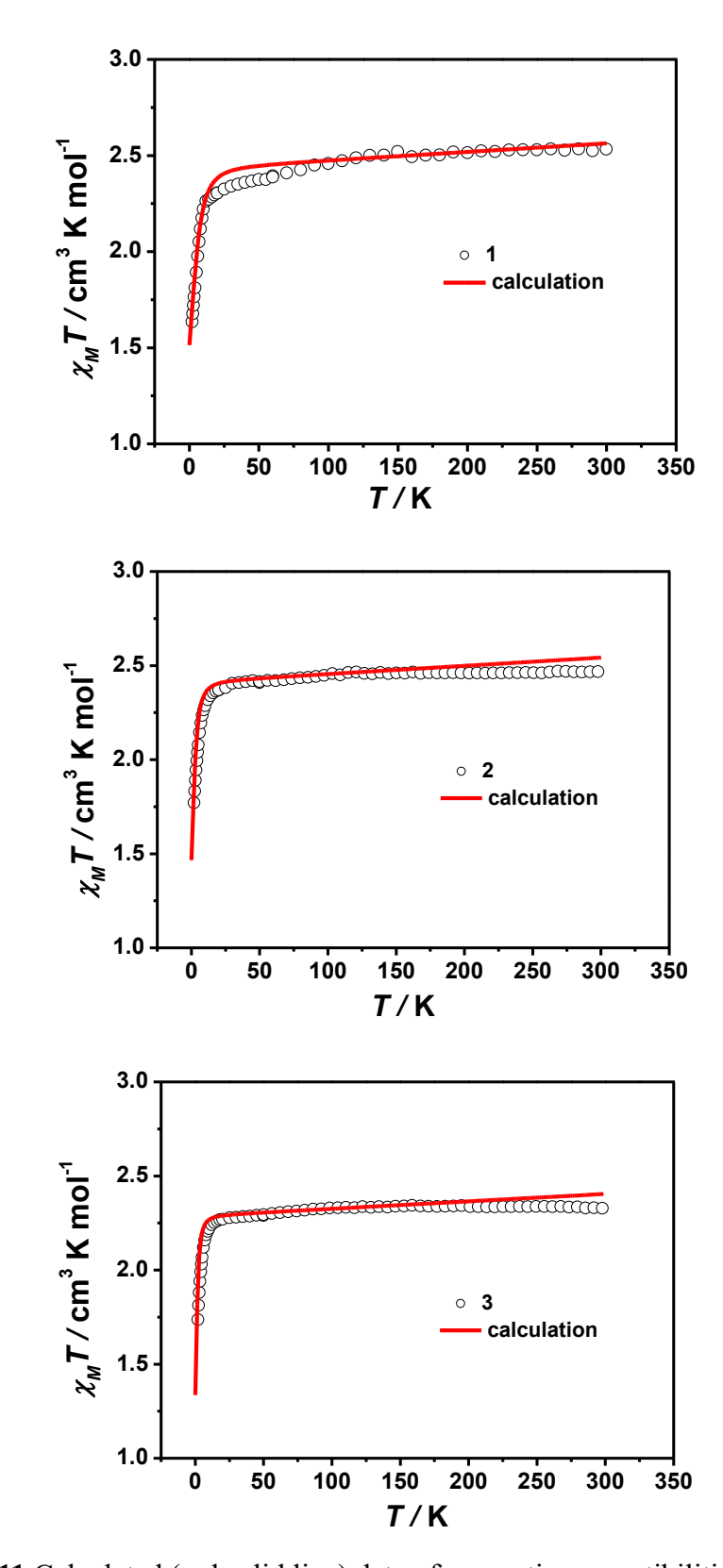


Fig. S11 Calculated (red solid line) data of magnetic susceptibilities of 1-3.

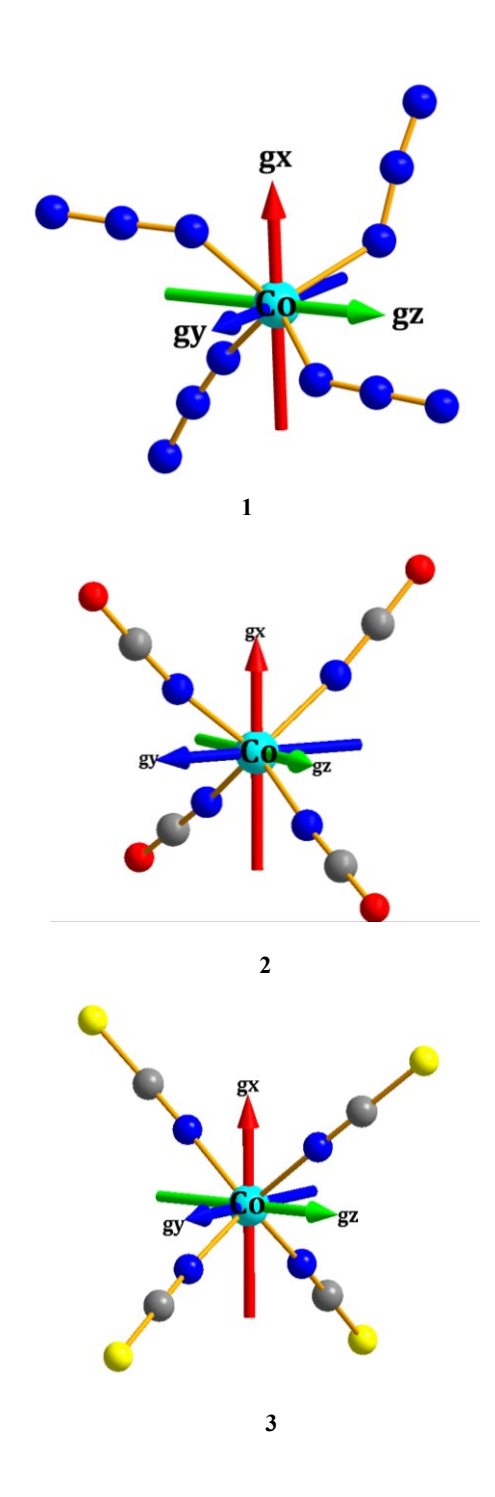


Fig. S12 Orientations of the local magnetic axes (red: g_x ; blue: g_y ; green: g_z) of the ground spin-orbit states on Co(II) ions of 1-3.

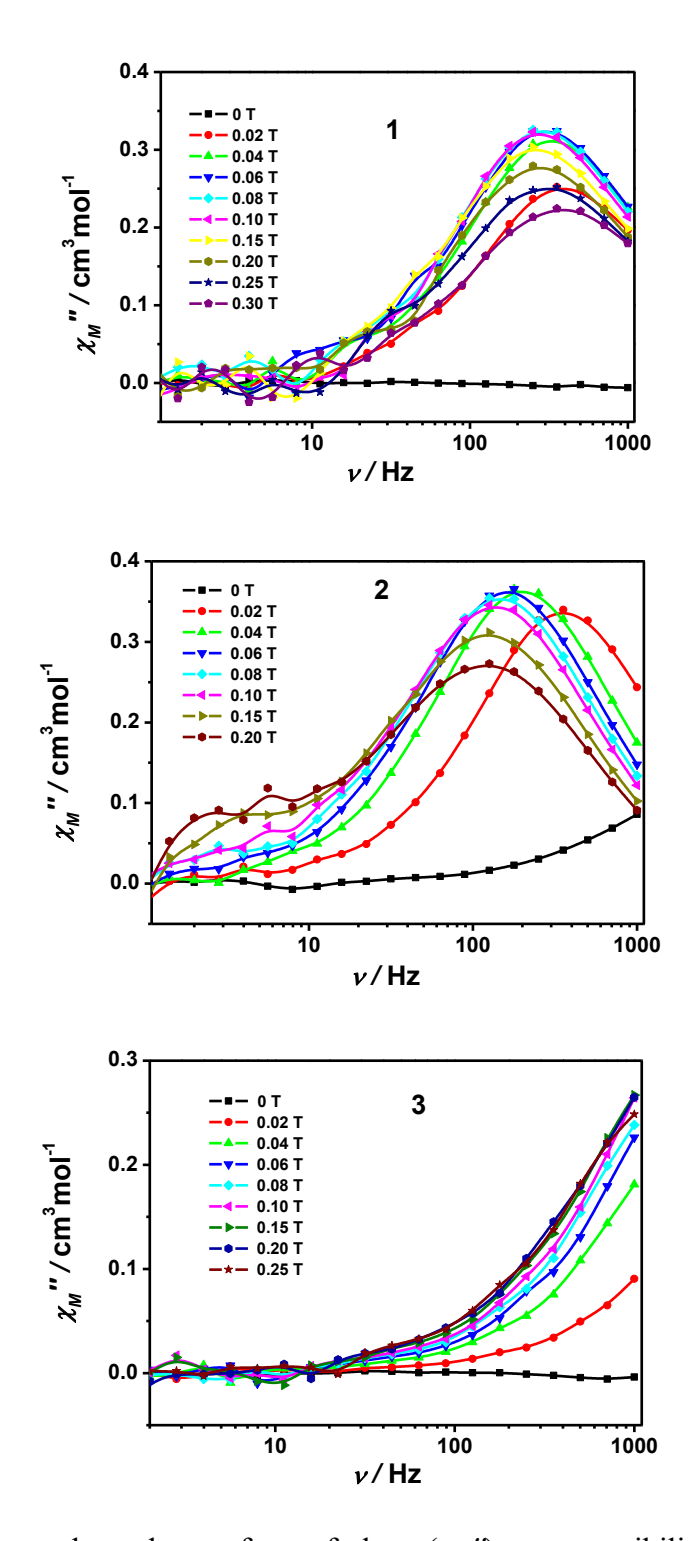


Fig. S13 Frequency dependence of out-of-phase (χ_M ") ac susceptibility at 1.8 K under the different applied static fields (from 0.02 to 0.30 T for 1, 0 to 0.20 T for 2, 0 to 0.25 T for 3). The solid lines are for eye guide.

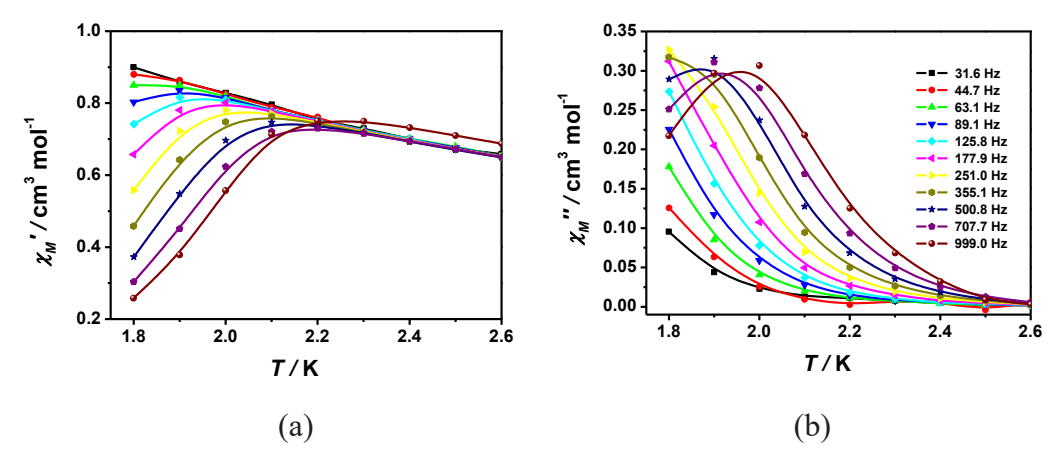


Fig. S14 (a) Temperature dependence of in-of-phase (χ_M ') and (b) out-of-phase ac susceptibility (χ_M '') at different ac frequency under a 0.08 T dc field for 1. The solid lines are for eye guide.

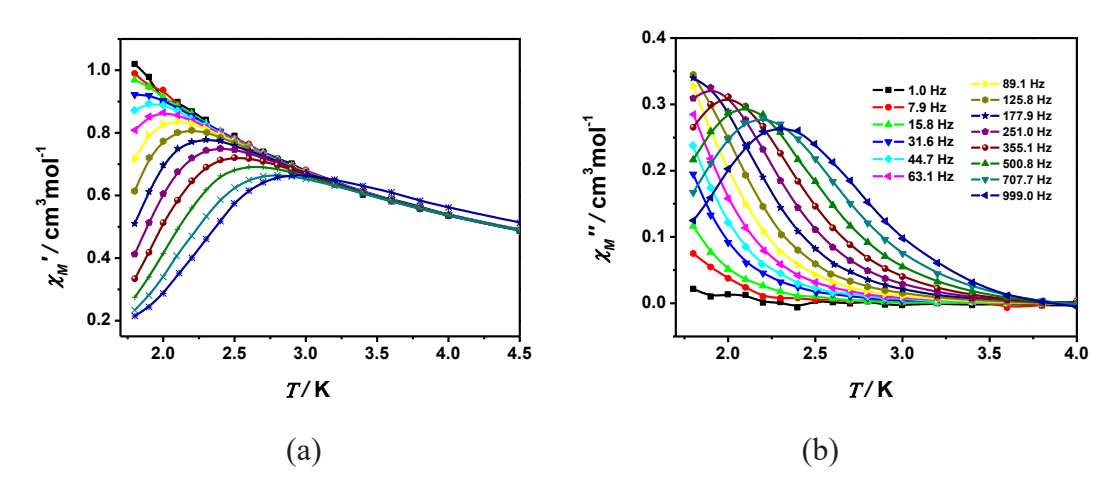


Fig. S15 (a) Temperature dependence of in-of-phase (χ_M ') and (b) out-of-phase ac susceptibility (χ_M ") at different ac frequency under a 0.1 T dc field for **2**. The solid lines are for eye guide.

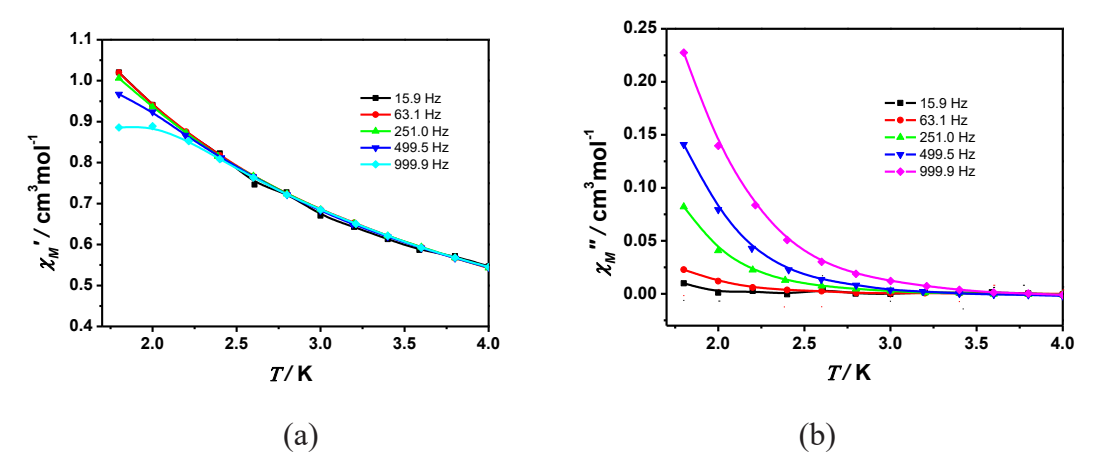


Fig. S16 (a) Temperature dependence of in-of-phase (χ_{M} ') and (b) out-of-phase ac susceptibility (χ_{M} ") at different ac frequency under a 0.1 T dc field for **3**. The solid lines are for eye guide.

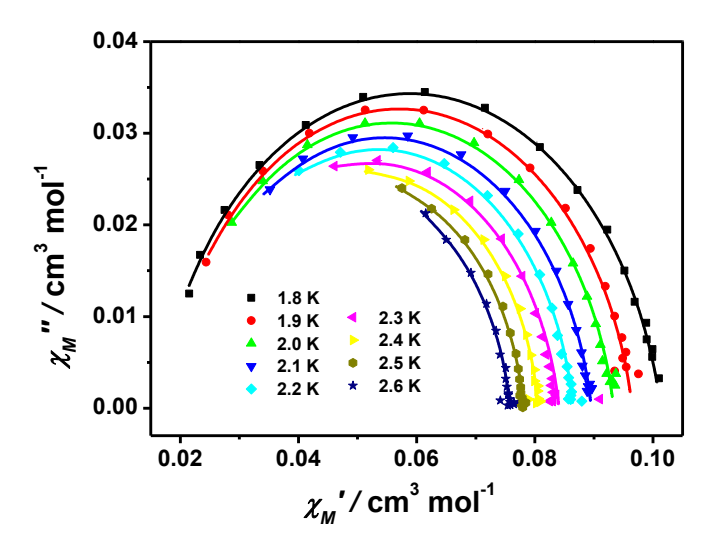


Fig. S17 Cole-Cole plot obtained from the ac susceptibility data under 0.1 T dc field between 1.8 and 2.6 K for **2**. Solid lines represent the best fits to a generalized Debye model.

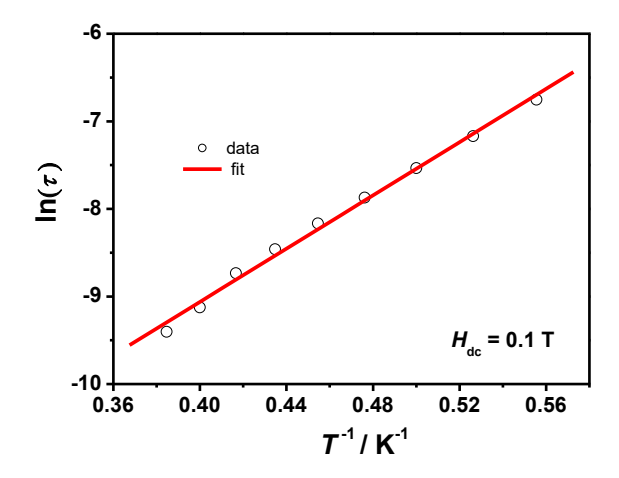


Fig. S18 Arrhenius plot for 2. The solid lines represent the best fit to the data.

Table S8 The parameters obtained by fitting the Cole-Cole plot under 0.1 T for 2

| T (K) | χs | χт | τ | α | Resi. |
|-------|---------|---------|--------------------------|-----------|--------------------------|
| 1.8 | 0.01639 | 0.10132 | 0.00117 | 0.126789 | 1.01607×10 ⁻⁵ |
| 1.9 | 0.01755 | 0.0965 | 7.69861×10 ⁻⁴ | 0.111988 | 2.29077×10 ⁻⁵ |
| 2.0 | 0.01821 | 0.09336 | 5.34053×10 ⁻⁴ | 0.111203 | 7.74388×10 ⁻⁶ |
| 2.1 | 0.01968 | 0.08955 | 3.81892×10 ⁻⁴ | 0.0984098 | 6.82749×10 ⁻⁶ |
| 2.2 | 0.02057 | 0.08646 | 2.84396×10 ⁻⁴ | 0.0892374 | 5.50196×10 ⁻⁶ |
| 2.3 | 0.02103 | 0.08407 | 2.11807×10 ⁻⁴ | 0.0963511 | 5.74912×10 ⁻⁵ |
| 2.4 | 0.02288 | 0.08055 | 1.62964×10 ⁻⁴ | 0.0695094 | 4.48526×10 ⁻⁶ |
| 2.5 | 0.02149 | 0.07806 | 1.18931×10 ⁻⁴ | 0.0781255 | 3.58249×10 ⁻⁶ |
| 2.6 | 0.01842 | 0.0758 | 8.34813×10 ⁻⁵ | 0.0893209 | 6.94129×10 ⁻⁶ |

References

- S1 J. M. Zadrozny, J. Telser and J. R. Long, *Polyhedron*, 2013, **64**, 209.
- S2 K.Chattopadhyay, M. J. H. Ojea, A. Sarkar, M. Murrie G. Rajaraman and D. Ray, *Inorg. Chem.*, 2018, 57, 13176.
- S3 M. Das, D. Basak, Z. Trávníček, J. Vančo and D. Ray, Chem. Asian J., 2019, 14, 3898.
- S4 J. M. Zadrozny and J. R. Long, J. Am. Chem. Soc., 2011, 133, 20732.
- S5 M. S. Fataftah, S. C. Coste, B. Vlaisavljevich, J. M. Zadrozny and D. E. Freedman, *Chem. Sci.*, 2016, 7, 6160.
- S6 M. S. Fataftah, J. M. Zadrozny, D. M. Rogers and D. E. Freedman, *Inorg. Chem.*, 2014, 53, 10716.
- S7 M. S. Fataftah, S. C. Coste, B. Vlaisavljevich, J. M. Zadrozny and D. E. Freedman, *Chem.* Sci., 2016, 7, 6160.
- S8 D. Tu, D. Shao, H. Yan and C. Lu, Chem. Commun., 2016, 52, 14326.
- S9 S. Vaidya, S. Tewary, S. K. Singh, S. K. Langley, K. S. Murray, Y. Lan, W. Wernsdorfer, G. Rajaraman and M. Shanmugam, *Inorg. Chem.*, 2016, **55**, 9564.

- S10 S. Sottini, G. Poneti, S. Ciattini, N. Levesanos, E. Ferentinos, J. Krzystek, L. Sorace and P. Kyritsis, *Inorg. Chem.*, 2016, 55, 9537.
- S11 X.-N. Yao, M.-W. Yang, J. Xiong, J.-J. Liu, C. Gao, Y.-S. Meng, S.-D. Jiang, B.-W. Wang and S. Gao, *Inorg. Chem. Front.*, 2017, 4, 701.
- S12 S. Tripathi, S. Vaidya, K. U. Ansari, N. Ahmed, E. Rivière, L. Spillecke, C. Koo, R. Klingeler, T. Mallah, G. Rajaraman and M. Shanmugam, *Inorg. Chem.*, 2019, 58, 9085.
- S13 Y. Rechkemmer, F. D. Breitgoff, M. van der Meer, M. Atanasov, M. Hakl, M. Orlita, P. Neugebauer, F. Neese, B. Sarkar, J. van Slageren, *Nat. Commun.*, 2016, 7, 10467.
- S14 Y. Shen, G, Cosquer, H. Ito, D. C. Izuogu, A. J. W. Thom, T. Ina, T. Uruga, T. Yoshida, S. Takaishi, B. K. Breedlove, Z.-Y. Li and M. Yamashita, *Angew. Chem. Int. Ed.*, 2020, 59, 2399.
- S15 E. Carl, S. Demeshko, F. Meyer and D. Stalke, Chem. Eur. J., 2015, 21, 10109.
- S16 J. Vallejo, E. Pardo, M. Viciano-Chumillas, I. Castro, P. Amorós, M. Déniz, C. Ruiz-Pérez, C. Yuste-Vivas, J. Krzystek, M. Julve, F. Lloreta and J. Cano, *Chem. Sci.*, 2017, 8, 3694.
- S17 H.-H. Cui, F. Lu, X.-T. Chen, Y.-Q. Zhang, W. Tong and Z.-L. Xue, *Inorg. Chem.*, 2019, **58**, 12555.
- S18 H. Bamberger, U. Albold, J. D. Midlíková, C.-Y. Su, N. Deibel, D. Hunger, P. P. Hallmen, P. Neugebauer, J. Beerhues, S. Demeshko, F. Meyer, B. Sarkar and J. van Slageren, *Inorg. Chem.*, 2021, 60, 2953.
- S19 R. Bruno, J. Vallejo, N. Marino, G. D. Munno, J. Krzystek, J. Cano, E. Pardo and D. Armentano, *Inorg. Chem.*, 2017, **56**, 1857.
- S20 C.-M. Wu, J.-E. Tsai, G.-H. Lee and E.-C. Yang, Dalton Trans., 2020, 48, 16813.
- S21 Y.-Y. Zhu, F. Liu, J.-J. Liu, Y.-S. Meng, S.-D. Jiang, A.-L. Barra, W. Wernsdorfer and S. Gao, *Inorg. Chem.*, 2017, **56**, 697.
- S22 A. Piecha-Bisiorek, A. Bieńko, R. Jakubas, R. Boča, M. Weselski, V. Kinzhybalo, A. Pietraszko, M. Wojciechowska, W. Medycki and D. Kruk, *J. Phys. Chem. A*, 2016, **120**, 2014.
- S23 O. Y. Vassilyeva, E. A. Buvaylo, V. N. Kokozay, B. W. Skelton, C. Rajnák, J. Titiš and R. Boča, *Dalton Trans.*, 2019, **48**, 11278.
- S24 Y.-Y. Zhu, F. Liu, J.-J. Liu, Y.-S. Meng, S.-D. Jiang, A.-L. Barra, W. Wernsdorfer and S. Gao, *Inorg. Chem.*, 2017, 56, 697.

- S25 R. Boča, J. Titiš, C. Rajnák and J. Krzystek, Dalton Trans., 2021, 50, 3468.
- S26 L. H. G. Kalinke, J. C. O. Cardoso, R. Rabelo, A. K. Valdo, F. T. Martins, J. Cano, M. Julve, F. Lloret and D. Cangussu, *Eur. J. Inorg. Chem.* 2018, 816.
- S27 J. Palion-Gazda, B. Machura, R. Kruszynski, T. Grancha, N. Moliner, F. Lloret, and M. Julve, Inorg. Chem. 2017, **56**, 6281.
- S28 D. Shao, L.-D. Deng, L. Shi, D.-Q. Wu, X.-Q. Wei, S.-R. Yang, and X.-Y. Wang, *Eur. J. Inorg. Chem.* 2017, 3862.
- S29 M. Llunell, D. Casanova, J. Cirera, P. Alemany and S. Alvarez, *SHAPE*, Version 2.1., Universitat de Barcelona, Barcelona, 2013.
- S30 N. F. Chilton, R. P. Anderson, L. D. Turner, A. Soncini and K. S. Murray, *J. Comput. Chem.*, 2013, 34, 1164.
- S31 F. Aquilante, J. Autschbach, R. K. Carlson, L. F. Chibotaru, M. G. Delcey, L. De Vico, I. Fdez. Galván, N. Ferré, L. M. Frutos, L. Gagliardi, M. Garavelli, A. Giussani, C. E. Hoyer, G. Li Manni, H. Lischka, D. Ma, P. Å. Malmqvist, T. Müller, A. Nenov, M. Olivucci, T. B. Pedersen, D. Peng, F. Plasser, B. Pritchard, M. Reiher, I. Rivalta, I. Schapiro, J. Segarra Martí, M. Stenrup, D. G. Truhlar, L. Ungur, A. Valentini, S. Vancoillie, V. Veryazov, V. P. Vysotskiy, O. Weingart, F. Zapata, R. Lindh, J. Comput. Chem., 2016, 37, 506.
- S32 L. F. Chibotaru, L. Ungur, A. Soncini, Angew. Chem. Int. Ed., 2008, 47, 4126.
- S33 L. Ungur, W. Van den Heuvel, L. F. Chibotaru, New J. Chem., 2009, 33, 1224.
- S34 L. F. Chibotaru, L. Ungur, C. Aronica, H. Elmoll, G. Pilet, D. Luneau, *J. Am. Chem. Soc.*, 2008, **130**, 12445.